Received: 5 May 2022 | Revised: 1 July 2022 | Accepted: 28 July 2022

DOI: 10.1002/hbm.26044

RESEARCH ARTICLE

WILEY

Activity flow mapping over probabilistic functional connectivity

Hengcheng Zhu[1] | Ziyi Huang[1] | Yifeixue Yang[1] | Kaiqiang Su[1] | Mingxia Fan[2] | Yong Zou[3] | Ting Li[4] | Dazhi Yin[1,4]

[1]Shanghai Key Laboratory of Brain Functional Genomics (Ministry of Education), School of Psychology and Cognitive Science, East China Normal University, Shanghai, China

[2]Shanghai Key Laboratory of Magnetic Resonance, School of Physics and Electronic Science, East China Normal University, Shanghai, China

[3]Institute of Theoretical Physics, School of Physics and Electronic Science, East China Normal University, Shanghai, China

[4]Shanghai Changning Mental Health Center, Shanghai, China

Correspondence
Dazhi Yin, School of Psychology and Cognitive Science, East China Normal University, 3663 North Zhong-Shan Road, 200062 Shanghai, China.
Email: dzyin@psy.ecnu.edu.cn

Funding information
"Technology Innovation 2030-Major Projects" on brain science and brain-like computing of the Ministry of Science and Technology of China, Grant/Award Number: 2021ZD0202600; National Natural Science Foundation of China, Grant/Award Numbers: 11835003, 31600869, 81471651; McDonnell Center for Systems Neuroscience; NIH Blueprint for Neuroscience Research

Abstract

Emerging evidence indicates that activity flow over resting-state network topology allows the prediction of task activations. However, previous studies have mainly adopted static, linear functional connectivity (FC) estimates as activity flow routes. It is unclear whether an intrinsic network topology that captures the dynamic nature of FC can be a better representation of activity flow routes. Moreover, the effects of between- versus within-network connections and tight versus loose (using rest baseline) task contrasts on the prediction of task-evoked activity across brain systems remain largely unknown. In this study, we first propose a probabilistic FC estimation derived from a dynamic framework as a new activity flow route. Subsequently, activity flow mapping was tested using between- and within-network connections separately for each region as well as using a set of tight task contrasts. Our results showed that probabilistic FC routes substantially improved individual-level activity flow prediction. Although it provided better group-level prediction, the multiple regression approach was more dependent on the length of data points at the individual-level prediction. Regardless of FC type, we consistently observed that between-network connections showed a relatively higher prediction performance in higher-order cognitive control than in primary sensorimotor systems. Furthermore, cognitive control systems exhibit a remarkable increase in prediction accuracy with tight task contrasts and a decrease in sensorimotor systems. This work demonstrates that probabilistic FC estimates are promising routes for activity flow mapping and also uncovers divergent influences of connectional topology and task contrasts on activity flow prediction across brain systems with different functional hierarchies.

KEYWORDS
activity flow mapping, cognitive control systems, dynamic framework, functional MRI, probabilistic functional connectivity, sensorimotor systems

1 | INTRODUCTION

An important challenge in neuroscience is to link the two forms of brain activity: task-evoked and spontaneous/intrinsic activities (Raichle, 2010). Earlier brain imaging (e.g., functional magnetic resonance imaging, fMRI) research-related specific cognitive processes to task-evoked activations and considered spontaneous brain activity as baseline or noise. Owing to the pioneering work of resting-state fMRI

(Biswal et al., 1995), an increasing number of studies have focused on spontaneous brain activity and have demonstrated that it has meaningful organizational architecture and functional relevance (Buckner & DiNicola, 2019; Deco et al., 2013; Power et al., 2014; Uddin, 2020). In particular, previous studies have shown high similarity in network structure during rest and the performance of different cognitive tasks (Cole et al., 2014; Smith et al., 2009). A plausible inference is that task-dependent reconfigurations of functional networks are shaped primarily by an intrinsic network architecture (Davison et al., 2015; Krienen et al., 2014). However, these studies cannot provide a mechanistic understanding of the relationship between task-evoked and intrinsic brain activities.

By training a mathematical model, Tavor et al. demonstrated that resting-state functional connectivity (FC) can predict individual variability in task activation maps (Tavor et al., 2016; Tik et al., 2021). More explicitly, recent studies have proposed a large-scale activity flow model that allows us to predict a variety of cognitive task activations via resting-state network connectivity (Cole et al., 2016; Ito et al., 2017). Briefly, the activation of a given region was predicted by the linear summation of the activations of all other regions weighted by their resting-state FC with the target region. This model can also be extended to predict dysfunctional task activations from disrupted resting-state FC in older adults (Mill et al., 2020) and patients with schizophrenia (Hearne et al., 2021). The activity flow mapping approach offers mechanistic insight into the relationship between resting-state network topology and task-evoked activation patterns and opens a new window into the large-scale information processing architecture of the human brain.

However, prior studies have mainly employed static, linear FC estimates (i.e., standard Pearson correlation and multiple regression approaches) as activity flow routes, assuming temporal stationarity across all resting-state scans. The Pearson correlation is the simplest and most frequently adopted method for estimating FC (Sanchez-Romero & Cole, 2021; Smith et al., 2013). The main disadvantage of this method is that it cannot distinguish between direct and indirect functional connections in the brain, thereby generating false positives. The work of Cole et al. has shown that multiple regression FC is superior to Pearson correlation estimation in activity flow prediction (Cole et al., 2016). This is because the multiple regression approach reflects more direct FC between regions by controlling signals from other regions. However, it should be noted that there are two potential drawbacks to the multiple regression approach. First, controlling all other regions when calculating a functional connection between two regions results in a reduction in the temporal degrees of freedom. Consequently, the length of fMRI scans (i.e., time series) limits the number of regions included in the multiple regression analysis. Second, multiple regression may lead to false negatives if a brain region is accidentally oversplit into two separate nodes (i.e., having collinear nodes; Bijsterbosch et al., 2017). Therefore, it is necessary to examine the influence of the length of fMRI scans on activity flow prediction.

Moreover, a growing number of studies emphasize that the brain is a dynamic system (Bassett & Sporns, 2017; Breakspear, 2017; Deco et al., 2011) and embodies time-varying reconfiguration of functional networks both at rest (Allen et al., 2014; Baker et al., 2014; Chang & Glover, 2010; de Pasquale et al., 2016; Vidaurre et al., 2017; Wang et al., 2021; Zalesky et al., 2014) and across different task contexts (Braun et al., 2015; Gonzalez-Castillo et al., 2015; Kucyi et al., 2018; Shine et al., 2016; Vatansever et al., 2015). Accumulating evidence suggests that time-resolved FC analysis (e.g., sliding window approach) may help extract more information about brain function than traditional static FC analysis, although challenges concerning analysis and interpretation remain (Hutchison et al., 2013; Keilholz et al., 2017). Specifically, resting-state FC dynamics are thought to reflect the brain's exploration of a rich and flexible repertoire of functional network configurations (Deco et al., 2013). Previous studies also indicated that both the strength and spatial distribution of intrinsic FC change dynamically and contribute to behavioral variability (Sadaghiani et al., 2015; Vidaurre et al., 2021). Therefore, it is plausible that an intrinsic network topology derived from a dynamic FC framework could serve as a promising representation of activity flow routes. This would advance our understanding of how distributed cognitive activations are coordinated by an intrinsic network topology that captures the dynamic nature of FC.

A potential assumption of the activity flow model is that neural activity propagates over distributed functional pathways. Previous studies have suggested that the function of each region is largely determined by its unique set of connections with the rest of the brain (Mars et al., 2018). For example, brain regions with connections distributed across multiple networks are defined as connector hubs, mainly included in higher-order cognitive control systems, such as the frontoparietal network (FPN). In contrast, regions with numerous within-network connections are considered provincial hubs that are primarily involved in primary sensorimotor systems (Bertolero et al., 2017). Further evidence indicates that the connectional topology of brain areas at rest is related to the functional activities of these regions during tasks (Bertolero et al., 2015; Chan et al., 2017). It is therefore important to test whether the between- and within-network connections of a region make an unbalanced contribution to activity flow prediction, which may provide mechanistic insight into the relationship between intrinsic connectional topology and functional roles of brain regions.

In addition, previous studies have indicated that correspondences between intrinsic and task-related functional architectures seem to vary across different task contrasts; that is, weak correspondence has been found for tight task contrasts (Mennes et al., 2013). Compared to loose task contrasts (i.e., using rest as the baseline), tight task contrasts refer to adopting appropriate control conditions and usually reflect higher-order cognitive processes more purely, such as in classic flanker attention task, incongruent versus congruent trials (tight task contrast), and incongruent/congruent trials versus rest baseline (loose task contrast). Accordingly, tight task contrasts may primarily be involved in higher-order cognitive control regions because primary sensorimotor processes are often well controlled. In contrast, both the sensorimotor and cognitive control regions were activated for loose task contrasts. Thus, examining the effect of task contrasts (tight vs. loose) on the performance of activity flow prediction across

different brain systems may help parse the mechanistic relationship between higher-order cognitive processes and functional systems.

In this study, we first proposed a new activity flow route derived from a dynamic brain network framework and tested it on the publicly available Human Connectome Project dataset (Van Essen et al., 2013). In contrast to the standard Pearson correlation and multiple regression FC approaches, we adopted our recently established probabilistic FC estimates as active flow routes (Yin et al., 2016, 2021; Yin, Zhang, et al., 2019), which refer to the occurrence frequency of the intrinsic functional connection between two regions across all temporal windows during rest. Although the representational form is also a single and fixed network connectivity matrix, probabilistic FC estimates have captured and carried dynamic brain connectivity information. For instance, while a functional connection between two regions is absent when using Pearson correlation across the whole scanning session, it may exist in certain temporal windows. Moreover, this probabilistic FC estimation is compatible with the perspective that the intrinsic function of a region is uncertain and is expressed in a probabilistic manner; its apparent function is detectable and deterministic only when specific cognitive tasks or stimuli are performed (Yin & Kaiser, 2021). Therefore, we hypothesized that probabilistic FC estimates derived from a dynamic framework may provide promising routes for transferring activity flows across a variety of distinct cognitive tasks.

To further test the effects of between- and within-network connections and tight versus loose task contrasts on the prediction of task-evoked activations across different functional systems, we subsequently performed activity flow mapping using between- and within-network connections separately for each brain region, as well as using a set of tight task contrasts. This can reveal the imbalance of distributed versus local information processing across different functional systems. We expected that between-network connections would show relatively high prediction performance in higher-order cognitive control systems compared to primary sensorimotor systems. Furthermore, for tight task contrasts, prediction accuracy would be improved in cognitive control systems, particularly in the FPN, because they play a dominant role in flexible cognitive control with global and distributed FC (Cole et al., 2013; Yin & Kaiser, 2021).

2 | MATERIALS AND METHODS

2.1 | The MRI dataset

The data we tested were part of the Washington University-Minnesota Consortium Human Connectome Project (HCP), that is, the commonly used "100 Unrelated Subjects" subset (main dataset), which excludes family relations and represents a sample of the general population (Van Essen et al., 2013). Consistently, this subset of data was selected for the seminal study of activity flow mapping (Cole et al., 2016). To further validate our main findings, another 100 unrelated subjects were also tested (replication dataset). Data collection was approved by the institutional review board of the individual site, and informed consent was obtained from each subject. Participants' average age was 29 years (ranging from 22 to 36), and 54% of them were female (for the validation dataset: average age was 28 years, ranging from 22 to 35, and 50% of them were female). This study was approved by the ethics committee of East China Normal University.

2.2 | Image acquisition

For the HCP dataset, the fMRI scans were acquired with a whole-brain multiband echo-planar imaging sequence and a 32-channel head coil on a modified 3 T Siemens Skyra MRI scanner. The sequence parameters are as follows: repetition time (TR) = 720 ms, echo time (TE) = 33.1 ms, flip angle = 52°, bandwidth = 2290 Hz/Px, in-plane field of view (FOV) = 208 × 180 mm^2, 72 slices, and 2.0 mm isotropic voxels, with a multiband acceleration factor of 8 (Ugurbil et al., 2013). Data were collected over 2 days. Each day, 28 min of rest (two runs, eyes open with fixation) fMRI data were collected, followed by 30 min of task fMRI (one run for each task) data collection. The seven tasks consisted of an emotion cognition task, a gambling reward task, a language task, a motor task, a relational reasoning task, a social cognition task, and a working memory task. The details of resting-state data collection can be found in previous study (Smith et al., 2013), as well as task data details (Barch et al., 2013).

2.3 | Data preprocessing

We used the minimally preprocessed volume version of the data. Standard procedures including spatial normalization to a standard template, motion correction, and intensity normalization had already been implemented (Glasser et al., 2013). One subject was excluded due to poor image quality in the orbitofrontal cortex. We performed further preprocessing using SPM (SPM12; http://www.fil.ion.ucl.ac.uk/spm) and REST software (Song et al., 2011). The specific steps for resting-state and task-state data preprocessing were as described below.

For the resting-state fMRI data, the first 10 volumes for each run were discarded for signal equilibrium and to allow participants' adaptation to the scanning environment. We also removed nuisance time series (motion estimates, cerebrospinal fluid and white matter signals) using linear regression. Note that we did not conduct global signal regression (GSR) in the main analysis, given the ongoing debate on this preprocessing step (Fox et al., 2009; Murphy et al., 2009). In particular, previous studies have suggested that the GSR may distort correlation matrices, especially for the dynamic FC analysis (Saad et al., 2012; Shen et al., 2015). However, a recent study has shown that motion artifacts is most strongly controlled with the GSR for dynamic FC analysis (Lydon-Staley et al., 2019). Therefore, we also performed a validation analysis with the inclusion of GSR in the preprocessing step. The linear trend was removed, and the data were temporally bandpass filtered (0.01–0.08 Hz) and spatially smoothed (full width at half maximum = 4 mm). For the task-state fMRI data,

motion estimates were removed from the time series using linear regression. The data were then spatially smoothed using a Gaussian filter at 4 mm.

2.4 | Resting-state network connectivity derived from static and dynamic frameworks

To construct network connectivity, we used a parcellation scheme composed of $N = 264$ putative functional areas (i.e., spherical regions of interest [ROIs] with a radius of 5 mm) (Power et al., 2011) to allow a direct comparison with the findings of seminal work (Cole et al., 2016). Importantly, this parcellation scheme provided explicit functional network assignments for all ROIs. Using the static framework, we consistently conducted two different FC estimates as activity flow routes, including standard Pearson correlation and multiple linear regression approaches (Cole et al., 2016; Ito et al., 2017). Briefly, the time series of each region was obtained by averaging the signals of all the voxels within the ROI. The Pearson correlation between each pair of time series across the whole resting scanning session was calculated, and Fisher's *z*-transformation was performed to allow the correlation values to be more normal. Therefore, a symmetric $N \times N$ FC matrix was generated for each participant. Notably, to maintain consistency with seminal work (Cole et al., 2016), we used both positive and negative correlations for activity flow mapping. Considering that the functional significance of negative correlations remains unclear, we also performed a validation analysis using only positive correlations.

In contrast, a multiple linear regression model was created to fit the time series of each to-be-predicted region separately by considering the time series of all other regions as covariates. The resulting betas (β_{ij}), a measure of the effect of the given source j contributing to target region i, are represented as alternative static FC estimates. Note that the multiple regression approach produced an asymmetric $N \times N$ FC matrix, which reflects the optimal linear scaling of the source time series to best match the target time series, instead of reflecting direction information.

We propose probabilistic FC estimates derived from a dynamic framework as new activity flow routes. Specifically, we first employed a popular sliding window method to construct dynamic FC matrices. Following previous studies (Liao et al., 2017; Yin et al., 2016), we used a tapered window (window length [WL] = 139 TRs ≈ 100 s) and slides in steps of one TR. However, to date, there is no universally accepted criterion for WL selection. Therefore, shorter and longer WLs (i.e., WL = 44 s and 150 s) (Allen et al., 2014; Liao et al., 2017) were also applied to validate our main findings. For each temporal window, the Pearson correlation between the mean time series of any pair of regions was computed, and a symmetric $N \times N$ connectivity matrix was obtained.

Subsequently, based on the dynamic FC matrices of each participant, we calculated the normalized probabilistic connectivity distribution $PC_i(j)$ for a given brain region i as follows (Yin et al., 2016, 2021; Yin, Zhang, et al., 2019):

$$PC_i(j) = \frac{n(c_{ij})}{k \times w}, j = 1, 2, \ldots N, \text{and } j \neq i,$$

where $n(c_{ij})$ denotes the number of times the connection between i and j emerged across the temporal windows, k is a predefined threshold indicating the number of the strongest connections (NSC) reserved for region i in each time window (because positive and negative correlations would imply a different flow in information, here we consider only positive correlations in our main analysis while taking absolute values only for a validation analysis), and w denotes the number of temporal windows. $PC_i(j)$ denotes the probability of occurrence of the connection between regions i and j across all temporal windows and ranges from 0 to 1. The greater the value of $PC_i(j)$, the more frequent the interaction between regions i and j across temporal windows, and vice versa.

Regarding the k threshold, we justified the choice of $k = 3$ for both human and monkey datasets in our previous studies (Yin et al., 2016; Yin, Zhang, et al., 2019). Therefore, we selected the same threshold, $k = 3$, for the main analysis and further validated our main findings with $k = 4$ and $k = 5$. In addition, it should be noted that the probabilistic FC matrices were asymmetric, which resulted from the local thresholding scheme (Alexander-Bloch et al., 2010) and not necessarily from the direction of the activity flow. This local thresholding scheme may allow the reduction of spurious connections owing to a short time window and enables the preservation of some important weak connections (compared with hard thresholding across the whole brain).

2.5 | Activity flow mapping over different resting-state network connectivity routes

In the current study, we performed activity flow mapping based on connectivity routes from both the static and dynamic frameworks. The basic idea of this model is that the cognitive task activation of a given region can be predicted by the linear summation of the activations of all other regions weighted by their resting-state FC with the target region. The formal mathematical formula is as follows (Cole et al., 2016):

$$P_j = \sum_{i \neq j \in V} A_i \cdot F_{ij},$$

where P_j is the predicted activation of region j in a given task contrast and A_i is the actual activation of region i in a given task contrast. F_{ij} is the FC estimate between regions i and j (here, FC represents the standard Pearson correlation, multiple regression FC estimate, or probabilistic FC estimate). Here, a total of 24 loose task contrasts (Table S1) were used following a recent study (Cole et al., 2021) and brain activation was estimated using a standard general linear model in SPM. Figure 1 illustrates the activity flow model with different connectivity routes.

To eliminate the scale effects of different task contrasts and subjects, the single-subject activation amplitudes for each task contrast

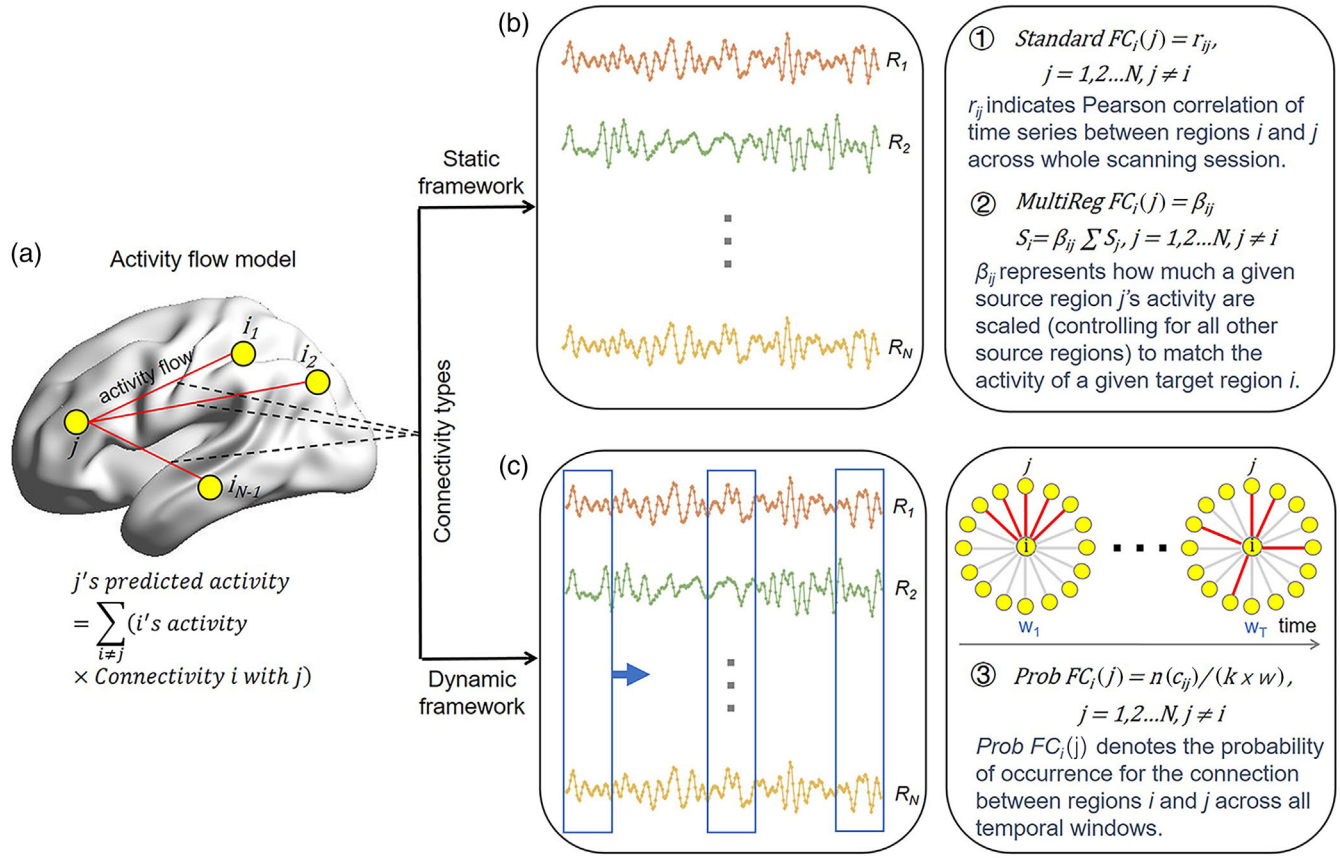

FIGURE 1 Standard, multiple regression, and currently proposed probabilistic FC routes for the activity flow model. (a) An illustration of the activity flow model. (b) Activity flow routes are estimated from the static framework using standard Pearson correlation and multiple regression FC approaches. S_i indicates the fMRI signal of region i. (c) Activity flow routes are estimated from the dynamic framework using probabilistic FC approach. $N(c_{ij})$ denotes the number of times the connection between regions i and j emerged across all temporal windows. K indicates the number of strongest connections reserved at each temporal window. W refers to the number of temporal windows. FC, functional connectivity; MultiReg, multiple regression; Prob, probabilistic; R, region

were z-normalized (subtracting the mean and dividing the standard deviation of the activation amplitude). The prediction accuracy was assessed based on the similarity between the predicted and actual activation values. Following a previous study (Cole et al., 2016), the predicted-to-actual correlation was computed across regions (within the entire brain or network) for each task contrast and then averaged across task contrasts. Considering that each network has a different number of regions, this may lead to a potential bias in the comparison of prediction accuracy across individual functional networks. To validate our main findings, we also computed the predicted-to-actual correlation across task contrasts for each region separately and then averaged across regions within the entire brain or network. However, this analytic strategy is inappropriate for examining the effect of tight versus loose task contrasts on the activity flow prediction for each network (or across the whole brain).

In addition, we conducted two assessment measures for the predicted-to-actual activation similarity: average-then-compare (r^*) and compare-then-average (r). The average-then-compare assessment, which had a better signal-to-noise ratio (SNR) but blurred single-subject information, was performed by calculating the similarity after averaging the predicted and actual activations across all subjects (i.e., group-level prediction). In contrast, the compare-then-average assessment, which focused on a single subject's distinctive prediction but with a low SNR, was performed by computing the Pearson correlation between predicted and actual activations for each subject separately, and these similarity estimates were then averaged across all subjects as the final prediction accuracy (i.e., individual-level prediction). Unless otherwise noted, all subsequent statistical analyses used the compare-then-average approach, enabling us to identify valid p-values (instead of focusing on average-then-compare assessment and using a permutation test).

2.6 | Effect of the length of resting-state scans on activity flow prediction with different FC approaches

In the main analysis, we used all four resting-state fMRI runs to estimate FC, following seminal work (Cole et al., 2016). Cole et al. found that multiple regression FC is superior to standard FC estimation in activity flow prediction. However, the multiple regression approach

would result in a reduction in the temporal degrees of freedom, and thus, might be more sensitive to the length of time points. Considering this, we further tested the effect of the length of resting-state scans on activity flow prediction using different FC approaches. For each FC approach, we first evaluated the consistency (or similarity) of the FC maps estimated using the main (four resting-state fMRI runs) and reduced (one resting-state fMRI run) datasets. We then performed activity flow prediction based on the FC routes estimated using the main and reduced datasets.

2.7 | Effect of applying a threshold to standard FC estimation on activity flow prediction

For probabilistic FC estimation, a threshold was applied, which may reduce the number of false connections (Yin et al., 2016). Similarly, although not using a threshold directly, multiple regression FC estimation may implicitly remove false connections by controlling for signals in all other regions (Cole et al., 2016). It would be helpful to determine whether activity flow prediction using the standard FC method improves when a threshold is applied. Therefore, we applied two representative thresholds (network sparsity $S = 0.15$ and 0.02) commonly used in brain network analyses (Liao et al., 2017; Power et al., 2011; Yin, Chen, et al., 2019) to the standard FC estimation for activity flow prediction.

2.8 | Identifying inter-subject specificity of activity flow prediction

To test the specificity of the model, we performed activity flow mapping for each participant by randomly selecting the FC routes of another participant in the group. The resulting predicted-to-actual correlations were considered null similarity estimates. The reason for not using the averaged FC across all subjects is that it may significantly increase the SNR. Because our goal was to identify the subject-specific effect of activity flow routes, the comparison between using an individual's own FC and another subject's FC was more reasonable.

2.9 | Effect of between- versus within-network connections on the activity flow prediction

Considering that the function of each region is largely determined by its unique connectional profiles, we performed activity flow mapping using between- and within-network connections separately for each brain region. The separate activity flow models are expressed as follows:

$$PB_j = \sum_{j \notin V_i} A_i \cdot F_{ij},$$

$$PW_j = \sum_{i \neq j \in V_i} A_i \cdot F_{ij},$$

where PB_j and PW_j denote the predicted activation of region j using between- and within-network connections, respectively; V_i denotes the functional network to which region i belongs; F_{ij} is the FC estimate between regions i and j. Similar to the main analysis with between- and within-network connections, PB_j and PW_j were calculated for each subject and for each task contrast using the three types of connectivity routes separately.

To further quantify the relative contribution of between- and within-network connections to activity flow prediction across different functional systems, the net rank (NR_i) of the prediction performance of between-network connections for functional system i is defined as follows:

$$NR_i = \frac{B_i}{(\sum B_i)/s} - \frac{W_i}{(\sum W_i)/s}, i = 1, 2, 3, \ldots, s,$$

where s represents the number of functional systems, and B_i and W_i denote the prediction accuracy of the functional system i using between- and within-network connections, respectively. An NR_i greater than zero indicates that between-network connections play a dominant role in activity flow prediction for functional system i. In contrast, an NR_i lower than zero indicates that within-network connections play a dominant role in the activity flow prediction for functional system i.

Considering that most of the seven tasks are primarily cognitive, we further tested whether there is a double dissociation effect, in which the sensorimotor system would show greater between-network connectivity contributing to the primary motor task. Specifically, for the primary motor task, we performed activity flow prediction using between- and within-network connections, separately for each brain region.

2.10 | Effect of tight versus loose task contrasts on the activity flow prediction

In the main analysis, all task contrasts were loose with rest as the baseline. To test how distinct types of task contrasts affect prediction accuracy across different functional systems, we additionally performed activity flow mapping for the six tight task contrasts (because no proper tight task contrast can be defined); here, we excluded the primary motor task from the seven tasks in the HCP dataset (Table S2). These tight task contrasts may reflect higher-order cognitive processes more purely with controlled primary sensorimotor processes, such as using the 2-back versus 0-back contrast for the working memory task. The analytical procedure for activity flow mapping was the same as that used in the main analysis.

2.11 | Statistical analysis

To investigate the prediction performance effects, we first conducted a two-way analysis of variance (ANOVA) with an FC type factor

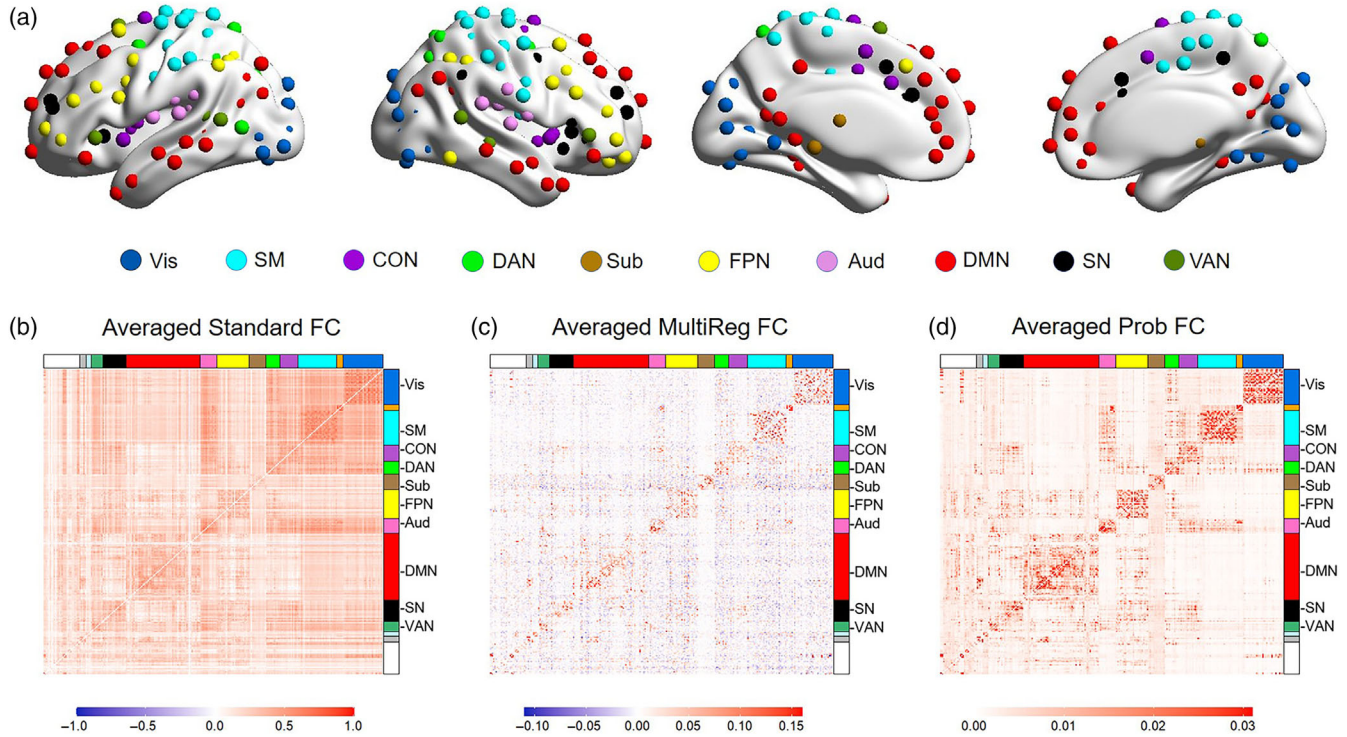

FIGURE 2 Brain parcellation and averaged network connectivity for each approach. (a) A commonly used functional parcellation (264 spherical regions of interest) with 10 well-known functional network assignments labeled with different colors. Based on this parcellation, averaged network connectivity was obtained with standard FC (b), multiple regression FC (c), and probabilistic FC (d) approaches. Aud, auditory network; CON, cingulo-opercular network; DAN, dorsal attention network; DMN, default mode network; FC, functional connectivity; FPN, frontoparietal network; MultiReg, multiple regression; Prob, probabilistic; SM, sensorimotor network; SN, salience network; Sub, subcortical network; VAN, ventral attention network; Vis, visual network

(standard FC vs. multiple regression FC vs. probabilistic FC) and a dataset type factor (4 vs. 1 resting-state fMRI run) at both whole-brain and individual-network levels. In the current study, we focused on 10 well-known functional systems (Figure 2a) for statistical analysis following previous studies (Cole et al., 2013; Cole et al., 2016; Yin, Chen, et al., 2019). Considering the effect of multiple comparisons, $p < .05$ with Bonferroni correction (i.e., $p < .05/11 = .0045$) was set as statistically significant. Post hoc analyses were performed to identify significant differences in prediction accuracy between FC types and between datasets.

To evaluate the effect of applying a threshold to standard FC estimation on activity flow prediction, we performed two-tailed two-sample *t*-tests between the prediction accuracy of applying a threshold of $S = 0.15$ (or 0.02) and that of using raw full connections. We considered $p < .05$ with Bonferroni correction (i.e., $p < .05/11 = .0045$) as statistically significant. To assess the specificity of activity flow mapping, we performed two-tailed two-sample *t*-tests for prediction accuracy using an individual's own and another subject's connectivity routes. We used $p < .05$ as statistical significance.

To examine the interaction effect between connectivity type and network type, we performed a two-way ANOVA with a connectivity type factor (between- vs. within-network connectivity) and a network type factor (10 different functional networks). We used $p < .05$ as statistical significance. To examine the separate contribution of between- and within-network connections to activity flow prediction for each functional system, we performed two-tailed two-sample *t*-tests between the prediction accuracy of using the between-network/within-network connections and that of using both. Furthermore, the net rank values of the prediction performance of between-network connections were contrasted with zero for each functional system using two-tailed one-sample *t*-tests. We considered $p < .05$ with Bonferroni correction (i.e., $p < .05/10 = .005$) as statistically significant.

To examine the interaction effect between contrast type and network type, we performed a two-way ANOVA with a contrast type factor (tight vs. loose) and a network type factor (10 different functional networks). We used $p < .05$ as statistical significance. To further compare the prediction accuracy of each functional network and whole-brain between tight and loose task contrasts, two-tailed two-sample *t*-tests were conducted. We considered $p < .05$ with Bonferroni correction (i.e., $p < .05/11 = .0045$) as statistically significant. To evaluate the effects of different NSC and WL thresholds, we first conducted a one-way ANOVA analysis for prediction accuracy at the levels of both the whole brain and individual functional networks. A threshold of $p < .05$ with Bonferroni correction (i.e., $p < .05/11 = .0045$) was set as statistically significant. Post hoc two-tailed two-sample *t*-tests were then carried out to compare the prediction accuracy using different thresholds.

3 | RESULTS

3.1 | Averaged network connectivity matrices of different activity flow routes

From the static and dynamic frameworks, we obtained three averaged network connectivity matrices representing the different types of activity flow routes (Figure 2b-d). The brain network constructed by standard FC showed strong within- and between-network connections, whereas the community structure was not very sharp (modularity $Q = 0.09$). In contrast, multiple regression FC and our currently proposed probabilistic FC networks presented a clearer community structure (modularity $Q = 0.27$ and 0.28 respectively) with relatively strong within-network connections and weak cross-network connections.

In addition, we found that similarity of the FC maps between using four and one resting state fMRI runs was as follows: $r^* = 0.99$ (average-then-compare) and $r = 0.83$ (compare-then-average) for standard FC estimation; $r^* = 0.76$ (average-then-compare) and $r = 0.25$ (compare-then-average) for multiple regression FC estimation; and $r^* = 0.99$ (average-then-compare) and $r = 0.76$ (compare-then-average) for probabilistic FC estimation (Figure S1). This result suggests that standard FC and probabilistic FC estimates are more robust to the lengths of fMRI scans than multiple regression FC estimates.

3.2 | Mean prediction accuracy estimated by average-then-compare and compare-then-average

Following the average-then-compare assessment, we found that using multiple regression FC routes led to higher prediction accuracy (mean $r^* = 0.93$) than using probabilistic (mean $r^* = 0.81$) and standard FC (mean $r^* = 0.71$) routes. In contrast, using probabilistic FC routes exhibited higher prediction accuracy (mean $r = 0.63$) than using multiple regression FC (mean $r = 0.58$) and standard FC (mean $r = 0.53$) routes based on compare-then-average assessment (Figure 3). Consistent findings were observed for individual task contrasts (Table S3). As suggested by previous studies (Cole et al., 2016, 2021), the overall increase in prediction accuracy for the average-then-compare assessment compared with the compare-then-average assessment likely benefits from its better SNR by averaging individual activations before prediction.

In addition, these findings have been consistently demonstrated in the replication dataset (for the average-then-compare assessment: mean $r^* = 0.93$ for multiple regression FC routes > mean $r^* = 0.82$ for probabilistic FC routes > mean $r^* = 0.71$ for standard FC routes; for the compare-then-average assessment: mean $r = 0.65$ for probabilistic FC routes > mean $r = 0.60$ for multiple regression FC routes > mean $r = 0.55$ for standard FC routes).

For the reduced dataset (using one resting-state fMRI run), we found that the multiple regression approach resulted in the lowest prediction accuracy with the compare-then-average assessment (mean $r = 0.57$ for probabilistic FC routes > mean $r = 0.48$ for standard FC routes > mean $r = 0.46$ for multiple regression FC routes), although it showed the highest prediction accuracy with the average-then-compare assessment (mean $r^* = 0.88$ for multiple regression FC routes > mean $r^* = 0.81$ for probabilistic FC routes > mean $r^* = 0.70$ for standard FC routes). The mean prediction accuracies estimated by both average-then-compare and compare-then-average methods are summarized in Table 1.

3.3 | Probabilistic FC routes significantly improved individual-level activity flow prediction compared with standard FC and multiple regression FC routes

Statistically, through two-way ANOVA, we found that both main (FC type, dataset type) and interaction (FC type × dataset type) effects were significant ($p < .05$, Bonferroni-corrected) at the levels of both the whole-brain and individual functional networks, except for the interaction effect of the subcortical network ($p < .05$, uncorrected) (Table S4). Post hoc analyses further revealed that probabilistic FC routes resulted in the highest prediction accuracy for the whole-brain network. At the level of individual functional networks, probabilistic FC routes produced the highest prediction accuracy for the SN (salience network), DMN (default mode network), and auditory networks. In contrast, multiple regression FC routes led to the highest prediction accuracy for the DAN (dorsal attention network) network. For the FPN, VAN (ventral attention network), CON (cingulo-opercular network), SM (sensorimotor network), and visual networks, the probabilistic FC and multiple regression FC routes showed comparable prediction performance, and both were better than the standard FC routes (Figure 4a). Notably, the subcortical network exhibited substantially low prediction accuracy for all three types of connectivity routes. These findings were consistent in the replication dataset (Figure S2). Compared with the main dataset (four resting-state fMRI runs), the reduced dataset (one resting-state fMRI run) resulted in a general reduction in the prediction accuracy for all three FC types (Figure S3). However, the reduction in prediction performance was more pronounced for the multiple regression FC approach, which showed the lowest prediction accuracy at the whole-brain network level (Figure 4b). This result suggests that the multiple regression FC approach is more sensitive to the reduction in data points in activity flow prediction.

3.4 | Effect of applying a threshold to standard FC estimation on activity flow prediction

When comparing full (raw) connections, we found that using the threshold of $S = 0.15$ did not lead to significant changes in prediction performance at either whole-brain or individual network levels. This result implies that weak connections play a trivial role in activity flow

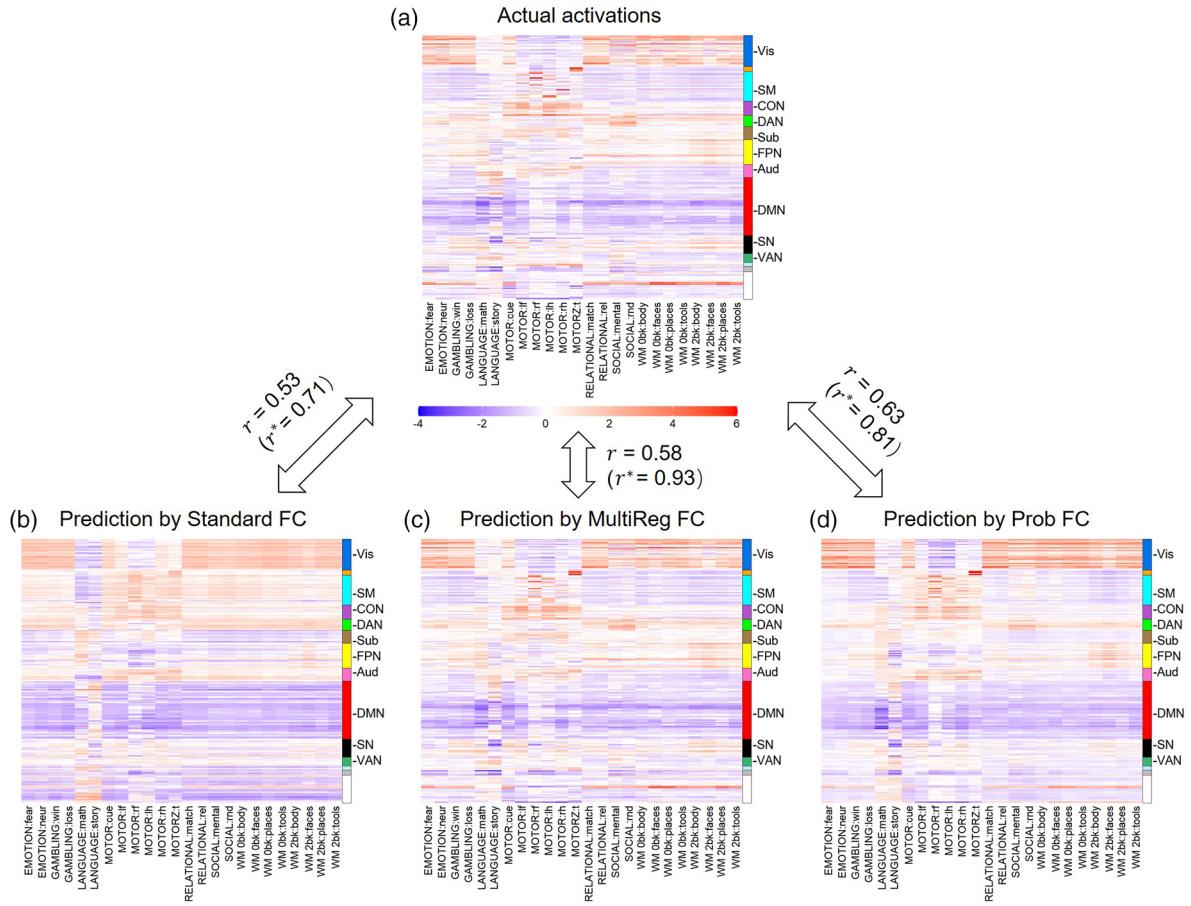

FIGURE 3 Mean similarity between actual activations (a) of 24 task contrasts and predicted activations (b-d) using different types of connectivity routes. *r* and *r** values denote compare-then-average and average-then-compare assessments, respectively. Aud, auditory network; CON, cingulo-opercular network; DAN, dorsal attention network; DMN, default mode network; FC, functional connectivity; FPN, frontoparietal network; MultiReg, multiple regression; Prob, probabilistic; SM, sensorimotor network; SN, salience network; Sub, subcortical network; VAN, ventral attention network; Vis, visual network

TABLE 1 Mean prediction accuracy for the three FC types with different datasets

	Main dataset		Replication dataset		Reduced dataset	
	r	(*r**)	*r*	(*r**)	*r*	(*r**)
Standard FC	0.53	0.71	0.55	0.71	0.48	0.70
MultiReg FC	0.58	0.93	0.60	0.93	0.46	0.88
Prob FC	0.63	0.81	0.65	0.82	0.57	0.81

Notes: *r* and *r** values denote compare-then-average and average-then-compare assessments, respectively. The replication dataset indicates the inclusion of another 100 unrelated subjects. The reduced dataset denotes that only one resting-state fMRI run is included, while the main and replication datasets include all four resting-state fMRI runs.
Abbreviations: FC, functional connectivity; MultiReg, multiple regression; Prob, probabilistic.

prediction. However, a significant reduction in prediction performance was observed at the whole-brain network level when using the threshold of $S = 0.02$, but showed opposite changes for the higher-order cognitive control (decreased) and primary sensory-motor (increased) networks (Figure 5). This finding suggests that using a very sparse threshold could improve the prediction performance of primary sensory-motor systems but reduce the prediction performance of higher-order cognitive control systems more prominently.

3.5 | Activity flow prediction dependent on individual-specific FC routes

To test inter-subject specificity, we conducted activity flow mapping for each subject using the connectivity routes of another subject in the group. For all three types of connectivity routes, we found that prediction accuracy using an individual's connectivity routes was significantly better (all *p* values <.001) than that using other connectivity

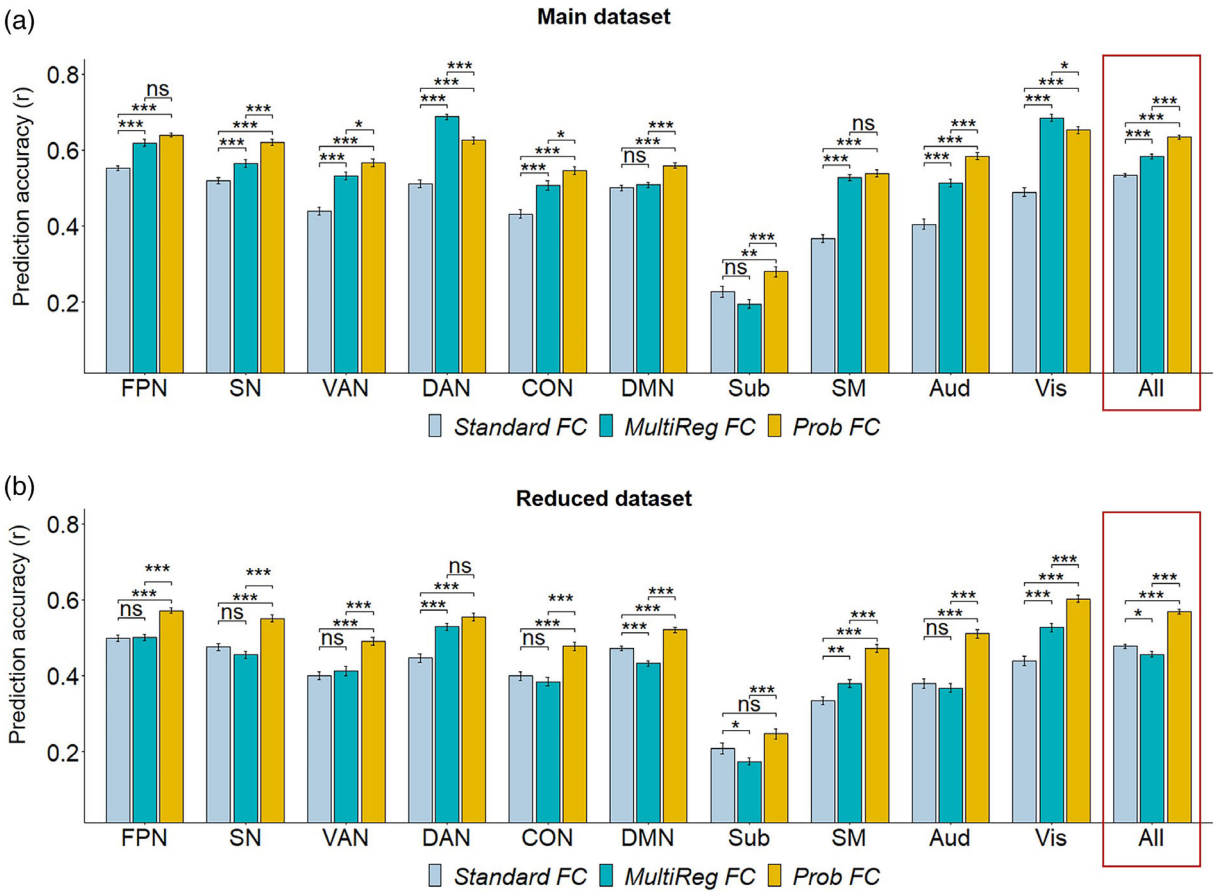

FIGURE 4 Statistical comparisons of prediction accuracy among using the three types of connectivity routes at the levels of both the whole-brain (All) and individual functional systems for the main (a, four resting-state fMRI runs) and reduced datasets (b, one resting-state fMRI run). Notably, while the predicted activation of each region is based on all other regions in the brain, the predicted-to-actual comparisons are only for each network. *p < .05; **p < .01; ***p < .001 (p < .05, Bonferroni-corrected); Aud, auditory network; CON, cingulo-opercular network; DAN, dorsal attention network; DMN, default mode network; FC, functional connectivity; FPN, frontoparietal network; MultiReg, multiple regression; *ns*, nonsignificant; Prob, probabilistic; SM, sensorimotor network; SN, salience network; Sub, subcortical network; VAN, ventral attention network; Vis, visual network

routes (Figure 6). This finding demonstrates that activity flow depends on individual-specific FC routes, suggesting the specificity of the activity flow mapping approach.

3.6 | The separate contribution of between- and within-network connections to activity flow prediction differs across functional systems

Through two-way ANOVA, we found that both main (connectivity type, network type) and interaction (connectivity type × network type) effects were significant (p < .001) for each FC approach (Table S5). For all three types of connectivity routes, we further observed that higher-order cognitive control networks (i.e., FPN, SN, VAN/DAN, and CON) showed a consistent reduction in prediction accuracy using either between- or within-network connections compared to using both (p < .05, Bonferroni-corrected). For the primary sensorimotor networks (i.e., SM, auditory, and visual), using between-network connections resulted in a remarkable decrease in prediction accuracy (p < .05, Bonferroni-corrected), whereas using within-network connections led to comparable or even enhanced prediction performance (Figure 7). This finding implies that both between- and within-network connections play a crucial role in activity flow prediction in higher-order cognitive control systems, whereas primary sensorimotor systems are largely dependent on within-network connections.

In addition, we found that between-network connectivity of the sensorimotor system consistently showed a lower contribution to activity flow prediction even for the motor task, while between-network connectivity of higher-order cognitive control networks remained more prominent (Table S6 and Figure S4). This result suggests that the effect of between- and within-network connections on the prediction of task-evoked activations across functional systems is largely dependent on intrinsic connectional profiles, rather than task types.

Quantitative assessment of the relative contribution of between- and within-network connections to activity flow

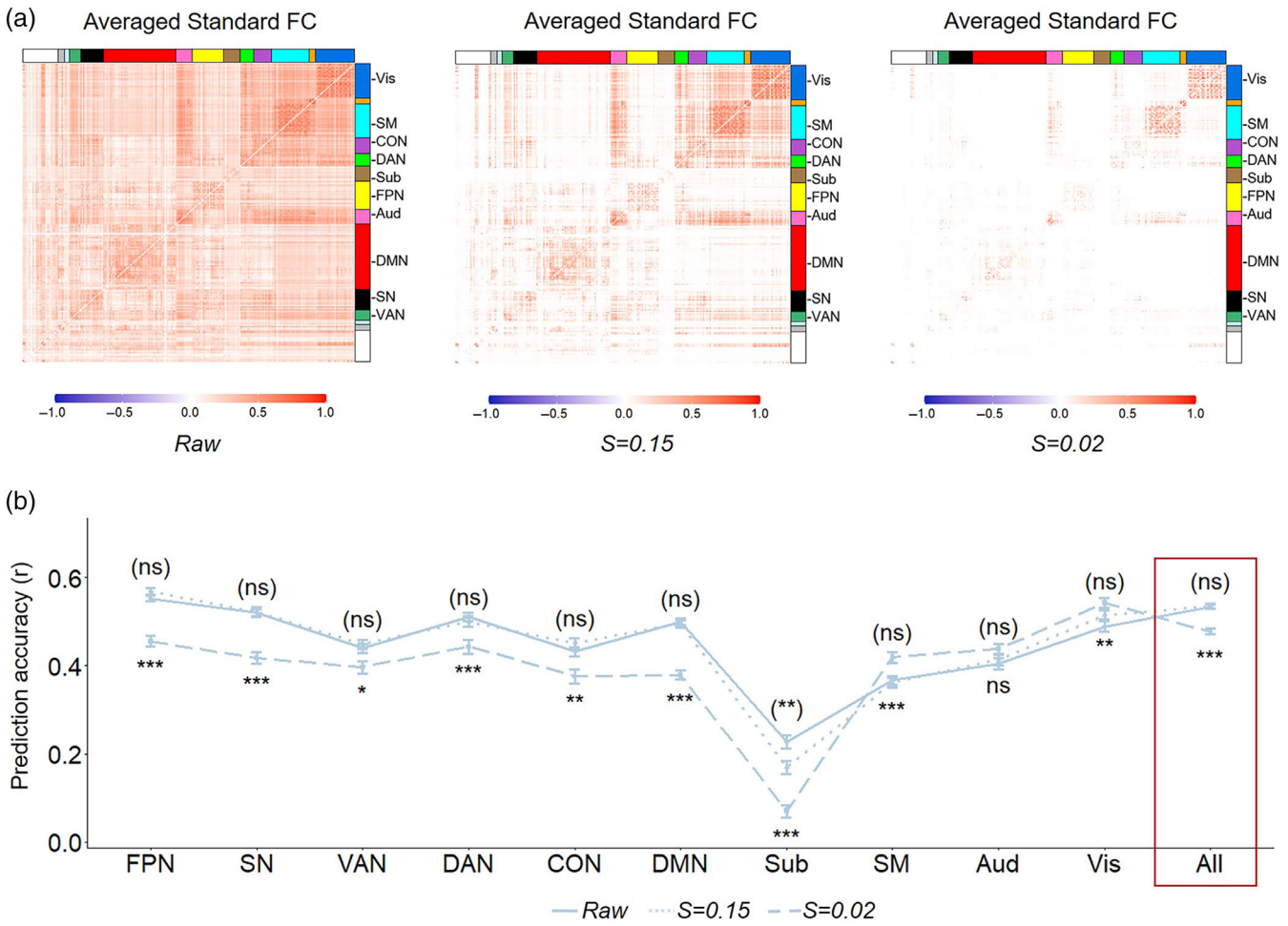

FIGURE 5 The effect of applying a threshold to standard FC estimation on activity flow prediction. Two representative thresholds (network sparsity $S = 0.15$ and 0.02) were selected to remove weak (false) connections, which are commonly used in brain network analyses. (a) Shows averaged network connectivity with different sparsity thresholds (left panel: Raw; middle panel: $S = 0.15$; right panel: $S = 0.02$). (b) Shows differences in prediction accuracy at the levels of both the whole-brain (All) and individual functional systems between using sparse and raw full network connections. Statistical significance with and without parentheses denote the differences for $S = 0.15$ versus raw and $S = 0.02$ versus raw, respectively. $^{*}p < .05$; $^{**}p < .01$; $^{***}p < .001$ ($p < .05$, Bonferroni-corrected); Aud, auditory network; CON, cingulo-opercular network; DAN, dorsal attention network; DMN, default mode network; FC, functional connectivity; FPN, frontoparietal network; MultiReg, multiple regression; *ns*, nonsignificant; Prob, probabilistic; SM, sensorimotor network; SN, salience network; Sub, subcortical network; VAN, ventral attention network; Vis, visual network

prediction across different functional systems revealed that the net rank of the prediction performance of between-network connections was consistently and significantly ($p < .05$, Bonferroni-corrected) greater than 0 for higher-order cognitive control networks (e.g., SN, DAN/VAN, and FPN) for all three types of FC routes. Conversely, the net rank of the prediction performance of between-network connectivity was significantly ($p < .05$, Bonferroni-corrected) lower than zero for the SM and visual networks (Figure 8). This result indicates that between-network connections play a more dominant role in activity flow prediction for higher-order cognitive control than primary sensorimotor systems. Instead, within-network connections have a relatively higher contribution to activity flow prediction for primary sensorimotor than higher-order cognitive control systems.

3.7 | Performance of distinct functional systems in activity flow prediction differs across tight and loose task contrasts

In addition to our main findings with 24 loose task contrasts, we applied an activity flow model to six tight task contrasts. For the averaged prediction accuracy, similar results were observed using the two sets of task contrasts, despite a slight overall decrease when using six tight task contrasts. Specifically, following the average-then-compare assessment, we found that multiple regression FC routes showed higher prediction accuracy (mean $r^* = 0.89$) than probabilistic FC (mean $r^* = 0.80$) and standard FC (mean $r^* = 0.71$) routes. In contrast, the probabilistic FC routes led to higher prediction accuracy (mean $r = 0.58$) than the multiple regression FC (mean $r = 0.52$) and

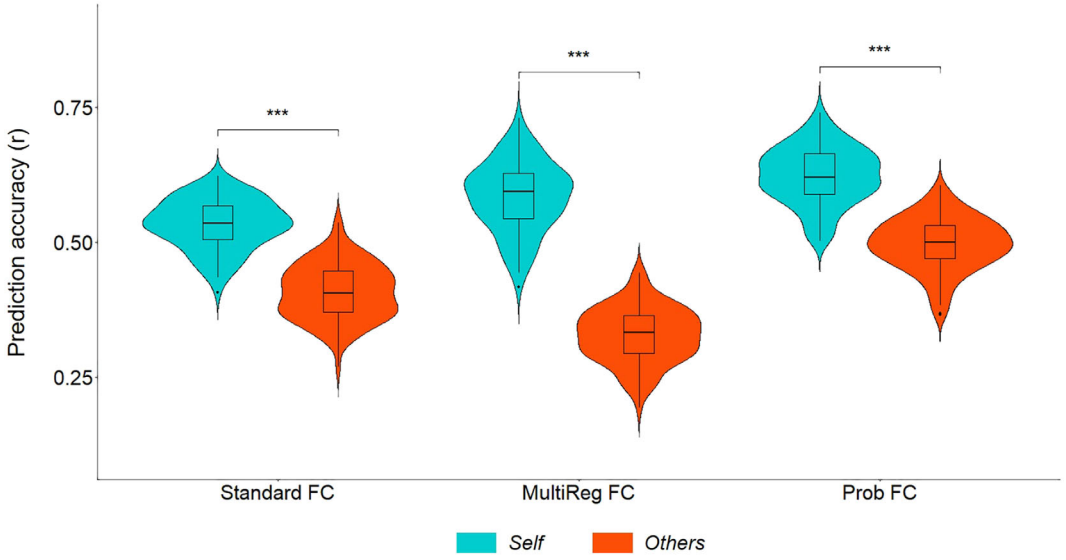

FIGURE 6 Specificity of the activity flow mapping approach. For all three types of connectivity routes (standard FC; MultiReg FC; and prob FC), prediction accuracy using individual connectivity routes was significantly better than that using other connectivity routes. ***$p < .001$; FC, functional connectivity; MultiReg, multiple regression; Prob, probabilistic

standard FC (mean $r = 0.50$) routes based on the compare-then-average assessment, which was consistent with the findings for individual task contrasts (Table S7). Statistically, we consistently found that probabilistic FC routes significantly improved individual-level activity flow prediction for the six tight task contrasts (Figure 9).

Through two-way ANOVA, we found that both main (contrast type, network type) and interaction (contrast type × network type) effects were significant ($p < .001$) for each FC approach, except for the main effect of contrast type using standard FC routes (Table S8). For all three types of connectivity routes, post hoc analyses showed that prediction accuracy at the whole-brain network level significantly ($p < .05$, Bonferroni-corrected) decreased for the tight task contrasts compared with the loose task contrasts. However, the prediction performance is substantially distinct across individual functional systems. Specifically, the higher-order cognitive control systems (i.e., FPN and SN) showed a significant increase in prediction accuracy for tight task contrasts compared with loose task contrasts; instead, a significant decrease was seen in the primary sensory systems (i.e., visual and auditory networks) (Figure 10). This result suggests that task contrasts (i.e., tight versus loose) have opposite effects on prediction accuracy across higher-order cognitive control and primary sensorimotor systems.

3.8 | Validation analyses

To test the effect of the GSR, we also performed activity flow prediction using all three FC types after applying the GSR. The average network connectivity obtained with the inclusion of GSR in the preprocessing step is shown in Figure S5. For standard FC, we found that prediction performance was slightly enhanced after GSR (with GSR: individual-level $r = 0.56$, group-level $r^* = 0.73$; without GSR: individual-level $r = 0.53$, group-level $r^* = 0.71$), which was consistent with a previous study (Cole et al., 2016). For multiple regression FC, we found that prediction performance remained the same after GSR (individual-level $r = 0.58$, group-level $r^* = 0.93$). Consistently, a previous study (Cole et al., 2016) claimed that multiple regression FC already implicitly removes the global signal by controlling for signals in all other regions. For probabilistic FC, we found that prediction performance was also slightly enhanced after GSR (with GSR: individual-level $r = 0.64$, group-level $r^* = 0.81$; without GSR: individual-level $r = 0.63$, group-level $r^* = 0.81$) (Figure S6). These findings indicate that our main conclusions are unchanged when GSR is included in the preprocessing step.

For the probabilistic FC approach, we also adopted the absolute values for activity flow prediction. Our results showed that prediction performance was slightly reduced using absolute values (individual-level $r = 0.62$, group-level $r^* = 0.81$) compared to using only positive correlations (individual-level $r = 0.63$, group-level $r^* = 0.81$) (Figure S7). For the standard FC approach, we consistently found that prediction performance was slightly enhanced using only positive correlations (individual-level $r = 0.54$, group-level $r^* = 0.71$) compared to using both positive and negative correlations (individual-level $r = 0.53$, group-level $r^* = 0.71$) (Figure S8). These findings suggest that negative correlations play a weak and negative role in activity flow prediction.

To test the potential influence of network size on cross-network comparisons, we conducted predicted-to-actual correlations across task contrasts for each region. We found that the differences in prediction accuracy when using different connectivity routes were consistent with our main findings, although the mean prediction accuracy slightly decreased (Figure S9). In addition, the effects

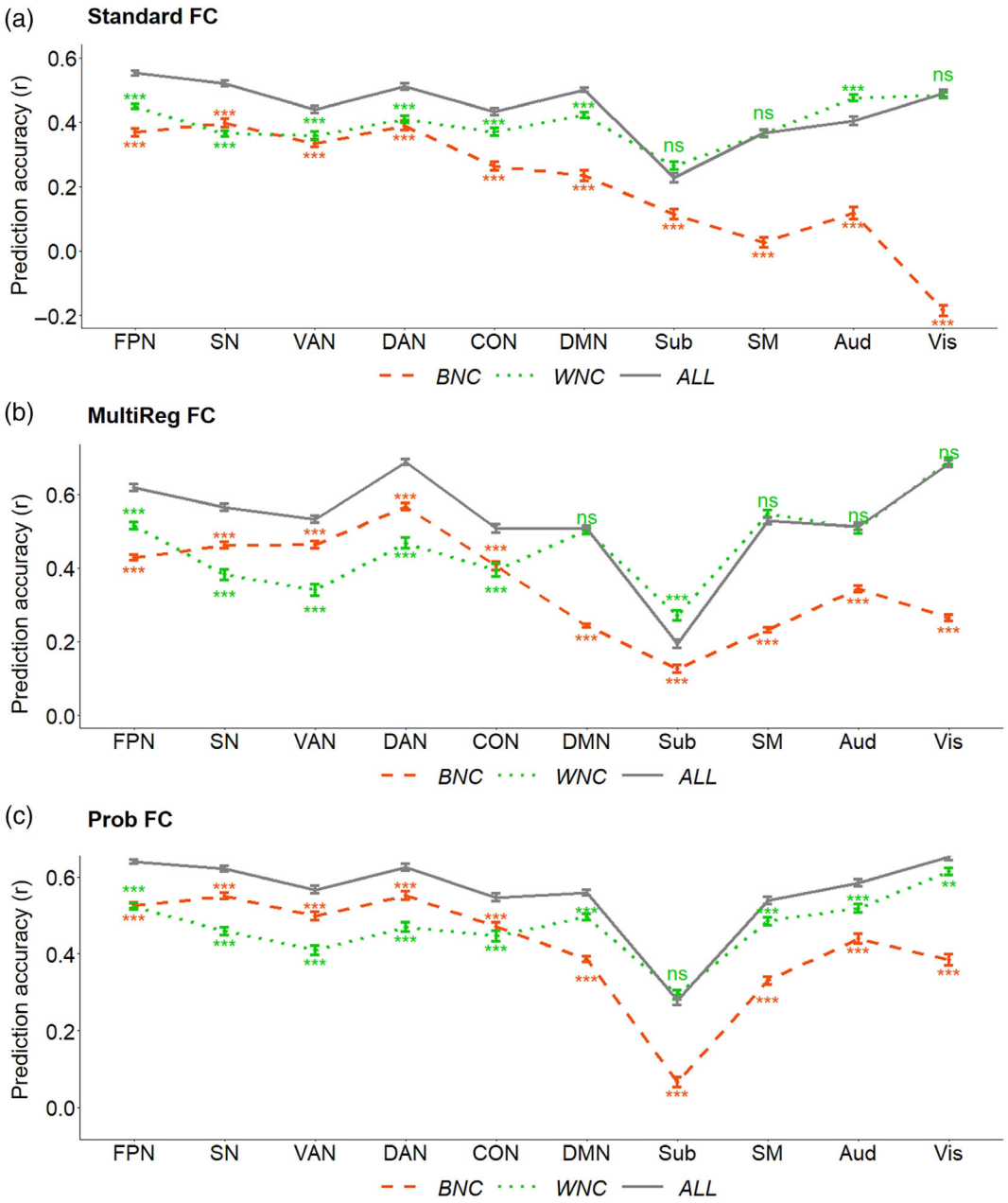

FIGURE 7 The effect of between- versus within-network connections on activity flow prediction across different functional systems for all three types of connectivity routes (a, standard FC; b, MultiReg FC; and c, prob FC). Activity flow prediction was performed using between- and within-network connections separately for each brain region and compared with using both (ALL). *$p < .05$; **$p < .01$; ***$p < .001$ ($p < .05$, Bonferroni-corrected); Aud, auditory network; BNC, between-network connections; CON, cingulo-opercular network; DAN, dorsal attention network; DMN, default mode network; FC, functional connectivity; FPN, frontoparietal network; MultiReg, multiple regression; *ns*, nonsignificant; Prob, probabilistic; SM, sensorimotor network; SN, salience network; Sub, subcortical network; VAN, ventral attention network; Vis, visual network; WNC, within-network connections

of between- and within-network connections on activity flow prediction across different functional systems were consistently observed (Figure S10). Although it was not significant for standard FC routes, the net rank of the prediction accuracy of between-network connections across functional systems was also consistently found using different connectivity routes (Figure S11). These results suggest that our main findings are robust to a predicted-to-actual correlation approach.

Using different NSC thresholds, ANOVA showed no significant differences in prediction accuracy at the levels of both the whole brain and individual functional systems (Figure S12 and Table S9). This result indicates that activity flow mapping with probabilistic FC routes is robust to different NSC thresholds. Using different WL thresholds, ANOVA revealed no significant difference in prediction accuracy at the levels of both the whole brain and individual functional systems (Figure S13 and Table S9). This result indicates that the activity-flow

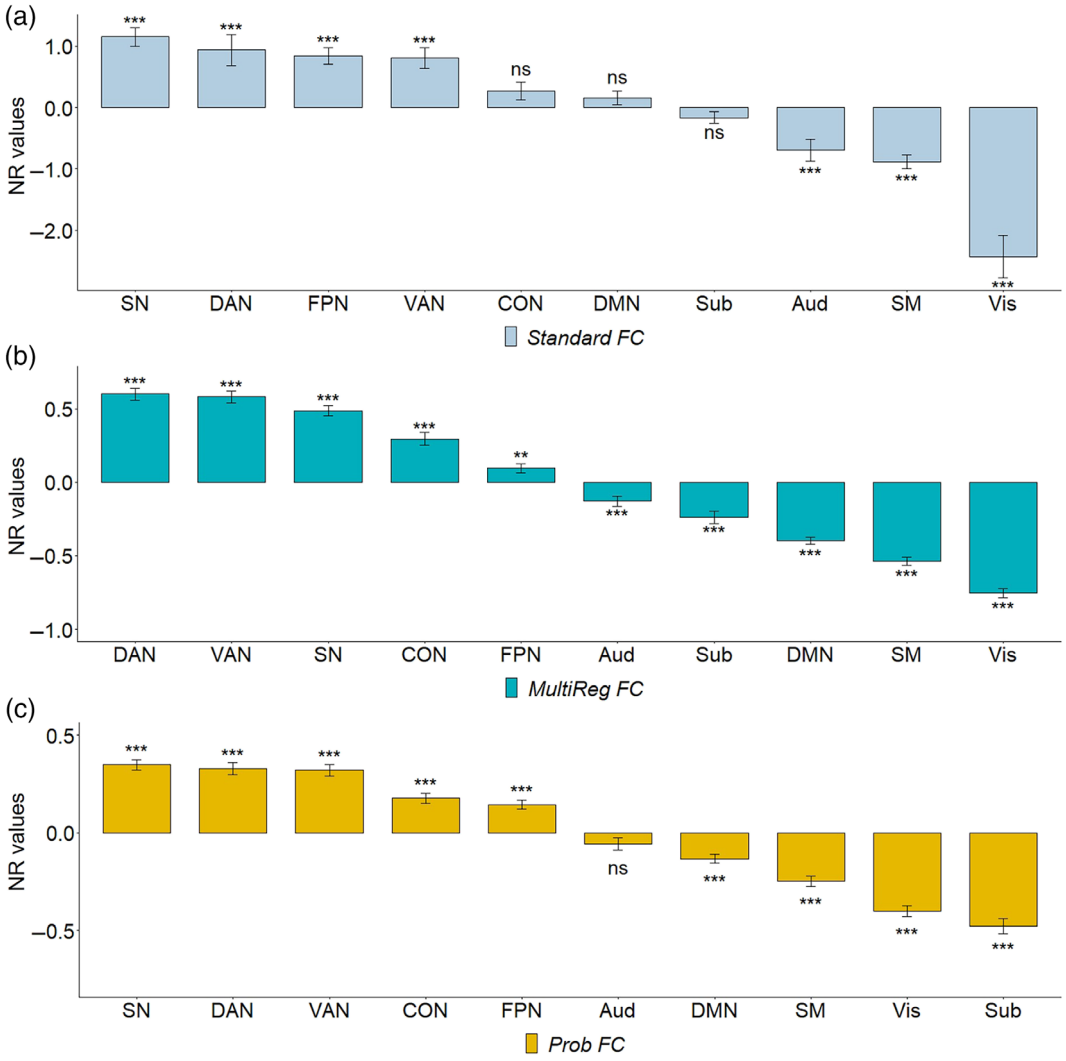

FIGURE 8 Net rank of prediction performance of between-network connections across functional systems using all three types of connectivity routes (a, standard FC; b, MultiReg FC; and c, prob FC). The net rank values greater than zero indicate that between-network connections play a more dominant role in activity flow prediction across functional systems. In contrast, net rank values lower than zero denote that within-network connections have a relatively higher contribution to activity flow prediction across functional systems. $^{*}p < .05$; $^{**}p < .01$; $^{***}p < .001$ ($p < .05$, Bonferroni-corrected); Aud, auditory network; CON, cingulo-opercular network; DAN, dorsal attention network; DMN, default mode network; FC, functional connectivity; FPN, frontoparietal network; MultiReg, multiple regression; *ns*, nonsignificant; Prob, probabilistic; SM, sensorimotor network; SN, salience network; Sub, subcortical network; VAN, ventral attention network; Vis, visual network

model with probabilistic FC routes is robust to different WL thresholds.

4 | DISCUSSION

Noninvasive brain imaging has provided a unique opportunity to investigate the functional organization of large-scale neural activity that underpins a variety of human cognitive processes. To uncover a mechanistic relationship between the two kinds of basic functional brain activities (i.e., intrinsic and evoked), recent studies have demonstrated a large-scale activity flow mapping approach to predict cognitive task activations by using resting-state network connectivity as routes (Cole et al., 2016; Ito et al., 2017). Considering that prior work mainly adopted static and linear network connectivity as activity flow routes, in this study, we presented a novel probabilistic FC route derived from a dynamic brain network framework. Moreover, we tested the effects of between- versus within-network connectivity routes and tight versus loose task contrasts on activity flow prediction, which can probe the imbalance in distributed versus local information processing across different functional systems. This study not only offered a new representation of activity flow routes but also further explored the influencing mechanisms of connectional topology and task contrasts on activity flow prediction across different functional systems.

Although multiple regression FC routes showed the best performance in group-level prediction, our proposed probabilistic FC routes substantially improved individual-level prediction. A previous study

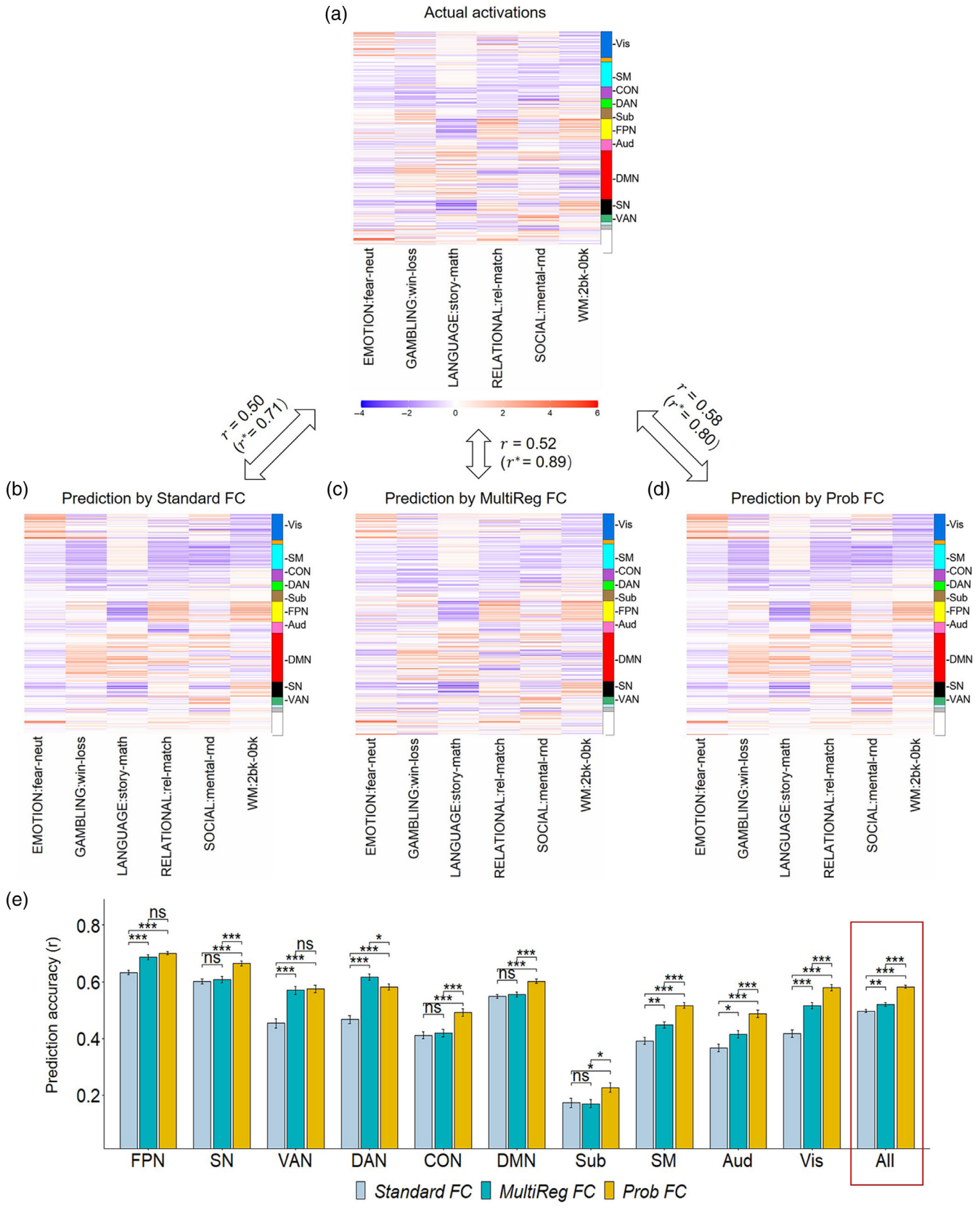

FIGURE 9 Legend on next page.

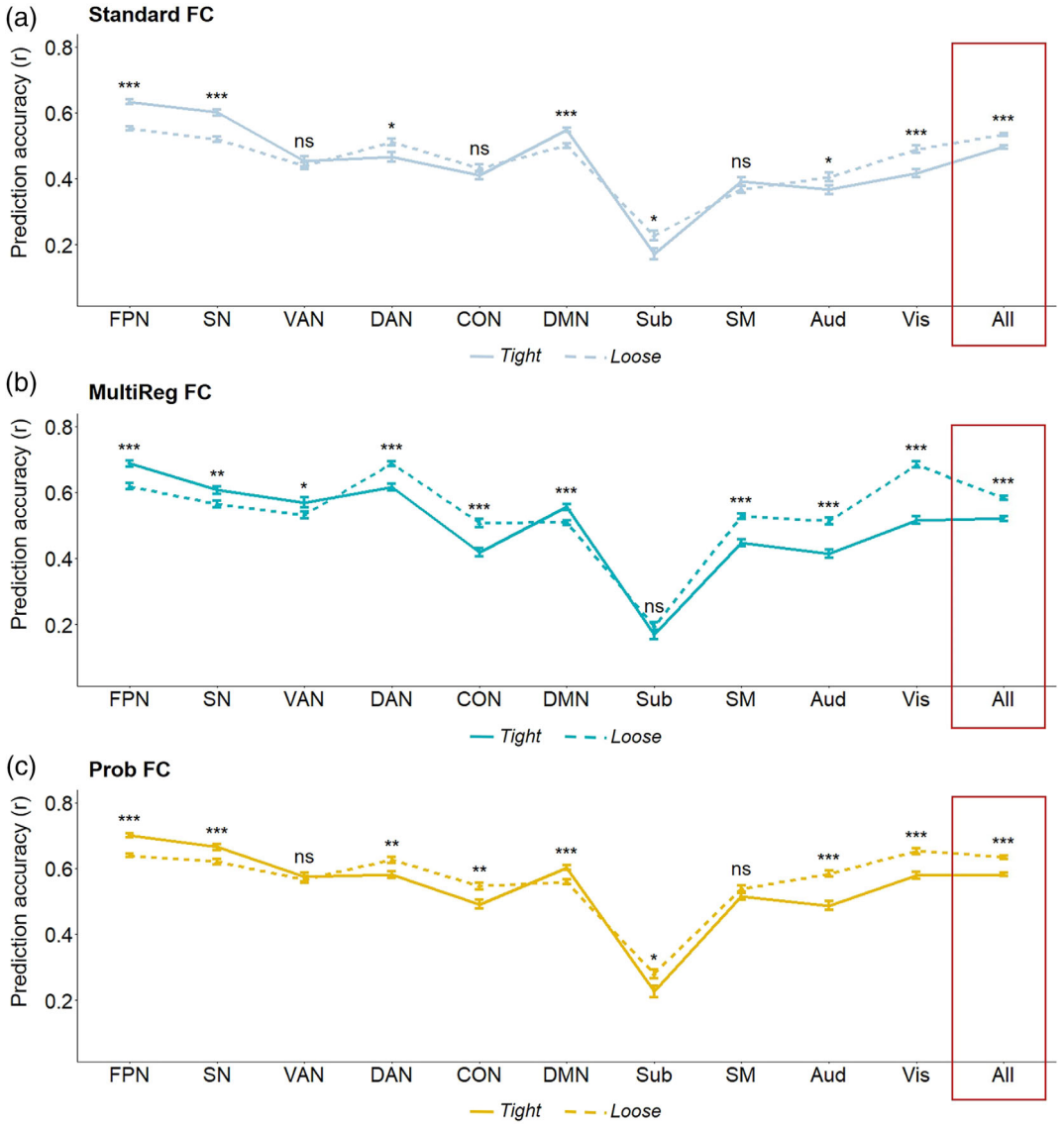

FIGURE 10 The effect of tight versus loose task contrasts on activity flow prediction across different functional systems. For all three types of connectivity routes (a, standard FC; b, MultiReg FC; and c, prob FC), prediction accuracy at the whole-brain network (All) level significantly decreased for the tight task contrasts compared with the loose task contrasts. However, the prediction performance is substantially distinct across individual functional systems. Specifically, the higher-order cognitive control systems showed a significant increase in prediction accuracy for tight task contrasts compared with loose task contrasts; instead, a significant decrease was seen in the primary sensory systems. $^{*}p < .05$; $^{**}p < .01$; $^{***}p < .001$ ($p < .05$, Bonferroni-corrected); Aud, auditory network; CON, cingulo-opercular network; DAN, dorsal attention network; DMN, default mode network; FC, functional connectivity; FPN, frontoparietal network; MultiReg, multiple regression; *ns*, nonsignificant; Prob, probabilistic; SM, sensorimotor network; SN, salience network; Sub, subcortical network; VAN, ventral attention network; Vis, visual network

has shown that multiple regression is superior to the standard FC approach for activity flow mapping because the former could reduce indirect FC between two regions by taking into account the effect of signals passing through a third region (Cole et al., 2016). Consistently, probabilistic FC was derived from a statistical measure of several of the strongest connections at each temporal window, which could

FIGURE 9 Mean similarity between actual activations (a) of the six tight task contrasts and predicted activations (b-d) using different types of connectivity routes. *r* and *r** values denote compare-then-average and average-then-compare assessments, respectively. (e) Statistical comparisons of prediction accuracy among using the three types of connectivity routes at the levels of both the whole-brain (All) and individual functional systems. $^{*}p < .05$; $^{**}p < .01$; $^{***}p < .001$ ($p < .05$, Bonferroni-corrected); Aud, auditory network; CON, cingulo-opercular network; DAN, dorsal attention network; DMN, default mode network; FC, functional connectivity; FPN, frontoparietal network; MultiReg, multiple regression; *ns*, nonsignificant; Prob, probabilistic; SM, sensorimotor network; SN, salience network; Sub, subcortical network; VAN, ventral attention network; Vis, visual network

reduce spurious connections to some extent (Yin et al., 2016). Therefore, compared to standard FC, we speculate that improved prediction of cognitive task activations is likely attributable to the fact that many indirect or artifact connections were removed by multiple regression and probabilistic FC approaches. Moreover, a recent study indicated that the time-varying nature of functional brain networks can explain some aspects of behavioral traits not captured by time-averaged FC or structural data (Vidaurre et al., 2021). It is possible that the improvement of individual-level activity flow prediction benefits from the dynamic nature of network interaction carried by the probabilistic FC routes. This may provide an important insight to the understanding of how the brain represents and coordinates information.

In comparison with the probabilistic FC approach, we also tested whether a threshold applied for the standard FC estimation can improve activity flow prediction. We found that using the threshold (network sparsity) of $S = 0.15$ did not lead to significant changes in prediction performance at either whole-brain or individual network levels. This result implies that weak connections play a trivial role in activity flow prediction. Moreover, it seems that activity flow can be sufficiently mapped using only 15% of the strongest connections (a network skeleton) of the brain, which also suggests the reasonability of usually taking sparse network connectivity to represent functional organization (Liao et al., 2017; Power et al., 2011; Yin, Chen, et al., 2019). However, a significant reduction in prediction performance was observed at the whole-brain network level when using the threshold of $S = 0.02$, but showed opposite changes for the higher-order cognitive control (decreased) and primary sensory-motor (increased) networks. This finding indicates that using a very sparse threshold could improve the prediction performance of primary sensorimotor systems, likely because of the removal of some strong but indirect within-network connections, but reduces the prediction performance of higher-order cognitive control systems more prominently. Together, our results indicate that a hard threshold applied to the standard FC estimation may not contribute to the improvement of activity flow prediction.

When comparing the main dataset (four resting-state fMRI runs, ~1 h), multiple regression FC routes produced the lowest individual-level prediction when using a reduced dataset (one resting-state fMRI run, ~15 min). This result suggests that the multiple regression FC approach is more sensitive to the length of data points. In line with this finding, a recent study showed that multiple regression FC led to a lower prediction accuracy than standard FC ($r = 0.46$ vs. $r = 0.51$) with a short time series (Cole et al., 2021). One explanation is that the multiple regression approach results in a reduction in the temporal degrees of freedom, which may result in a salient effect for a short time series. Furthermore, compared with the standard Pearson correlation, multiple regression FC estimations, considering a set of nodes, can amplify noise, particularly using noisy and few data points (Bijsterbosch et al., 2017). This is probably why the multiple regression approach shows a higher group-level prediction (improved SNR). In addition, most of the studies (especially for patients) are merely allowed to collect about 10-min resting-state fMRI scans, not as much as the HCP data (i.e., four resting-state fMRI runs, ~1 h). Therefore, our work is likely helpful in selecting proper FC methods according to the length of the fMRI scans.

By testing the effect of areal connectivity profiles on activity flow mapping, our findings indicate that both between- and within-network connections make a crucial contribution to activity flow prediction in higher-order cognitive control systems, whereas primary sensorimotor systems are primarily dependent on within-network connections. Both modeling and empirical studies have shown that large-scale brain networks are topologically organized with communities and hubs to promote the segregation and integration of neural information (Deco et al., 2015; Sporns, 2013; Zamora-Lopez et al., 2010). These hubs can be further divided into different types in terms of their connectional profiles (Guimera & Nunes Amaral, 2005; van den Heuvel & Sporns, 2013). Accordingly, a disproportionate number of connectors and provincial hubs have been identified across different functional systems; for example, higher-order cognitive control systems include many more connector hubs, while primary sensorimotor and DMN systems are mainly occupied by provincial hubs (Bertolero et al., 2017; Betzel et al., 2018; Power et al., 2013). Notably, although the DMN belongs to higher-order association systems, most regions are provincial hubs with many intra-network connections. Owing to the existence of many connector hubs in cognitive control systems, both between- and within-network connections contribute to activity flow prediction. In contrast, because there are few connector hubs, activity flow prediction in sensorimotor and DMN systems is largely determined by within-network connections. In addition, sensorimotor systems are strongly modular compared with higher-order cognitive control networks and exhibit very weak between-network connectivity. This may explain why the within-network connectivity of sensorimotor systems has a higher contribution. We found that between-network connectivity of the sensorimotor system showed a lower contribution to activity flow prediction even for the motor task, while the between-network connectivity of higher-order cognitive control networks remained more prominent. Together, our findings suggest that the effect of between- and within-network connections on the prediction of task-evoked activations across functional systems is largely dependent on intrinsic connectional profiles, rather than task types.

Across functional brain systems, we further quantified that between-network connections play a more dominant role in activity flow prediction for cognitive control systems than for sensorimotor systems. Instead, within-network connections have a relatively higher contribution to activity flow prediction for sensorimotor systems than for cognitive control systems. This finding indicates a gradient of distributed versus local neural processing across the functional systems. Many studies have suggested that cognitive control areas usually flexibly update their global FC to support adaptive task demands, while sensorimotor areas are mainly connected within their communities to achieve specific functions (Bertolero et al., 2018; Chen et al., 2016; Cole et al., 2013; Liao et al., 2017). Convergent evidence implies that unbalanced local and distributed processing across functional systems is associated with the brain hierarchy or gradient organization (Huntenburg et al., 2018; Margulies et al., 2016). Ito et al. reported a

negative relationship between localized and distributed processes across the cortical functional hierarchy (Ito et al., 2020). In line with this framework, our results offer new insights into a functional hierarchy based on activity flow prediction with between- and within-network connections.

Regarding the effect of tight versus loose task contrasts on activity flow mapping, we observed a significant decrease in prediction accuracy at the whole-brain network level using tight compared with loose task contrasts. This overall reduction is likely due to the smaller number of tight task contrasts (i.e., 6 tight vs. 24 loose task contrasts). Interestingly, at the level of individual functional networks, we found that higher-order cognitive control networks (i.e., FPN and SN) showed a remarkable increase in prediction accuracy in tight task contrasts compared to loose task contrasts and a significant decrease in primary sensory networks. A rough distinction between loose and tight task contrasts is that the former may activate both primary sensory and higher-order cognitive control areas, while the latter recruits cognitive control areas more purely because sensory stimulus-driven processing is often well controlled. Hence, the decline in prediction accuracy in sensory areas is possibly a result of their activations being reduced in tight task contrasts, which is equivalent to a decrease in the SNR.

On the other hand, activations of cognitive control areas may be involved in both top-down and bottom-up processes in loose task contrasts, while tight task contrasts may primarily account for the top-down process. Cognitive processes comprise complex interactions between primary sensory and cognitive control systems through feedforward and feedback connections (Corbetta & Shulman, 2002; Engel et al., 2001; Kastner & Ungerleider, 2000). In particular, previous studies have suggested that the modulation strength of activity between cognitive control and primary sensory areas depends on stimulus contrast (Ekstrom et al., 2008; Roelfsema, 2006). Therefore, we speculate that the improved prediction accuracy in cognitive control areas is likely attributable to the more specific and refined activity flow that occurred in the tight task contrasts.

Although our proposed probabilistic FC routes showed superior performance in individual-level activity flow prediction, a few methodological issues should be considered. First, despite the commonly used sliding window approach adopted to characterize dynamic FC, it is potentially affected by the general limitations of this technique (Hindriks et al., 2016; Hutchison et al., 2013). Specifically, although the HCP datasets using multiband acquisition could dramatically improve the sampling rate, some spurious correlations remain because of the relatively few data points for each time window or low SNR in subcortical areas. To reduce the effect of artifact connections, we calculated probabilistic FC using a statistical assessment of only a few of the strongest connections for each region in each temporal window. In addition to the benefit of removing potentially spurious connections, the local thresholding method (Alexander-Bloch et al., 2010) can preserve some important weak connections in comparison with hard thresholding methods based on whole-brain connections.

Second, both current and previous studies have employed the same linear activity flow model for different brain functional systems, despite multiple FC routes being tested. However, our findings showed divergent effects of areal connectivity topology and task contrast on activity flow prediction, at least between higher-order cognitive control and primary sensorimotor systems. Computational simulations also imply that activity flow mapping is more suitable for describing global information processing (Cole et al., 2016). In addition, to conduct a fair comparison of single FC approaches, we did not perform activity flow mapping with combined FC routes (Sanchez-Romero & Cole, 2021) in this study, although they may improve activity-flow prediction. Therefore, it would be interesting for future studies to explore the difference in activity flow mechanisms between functional systems with adjusted models (e.g., nonlinear) or advanced connectivity routes (e.g., causal FC [Reid et al., 2019]).

Third, following a previous study (Cole et al., 2016), prediction accuracy (or predicted-to-actual correlation) was computed across regions for each task contrast and then averaged across task contrasts. This may lead to potential bias in the comparison of prediction accuracy across individual functional networks. However, by computing predicted-to-actual correlations across task contrasts for each region separately, consistent results were obtained. Moreover, the goal of the current study was to compare the prediction performance using different connectivity routes, connectional profiles, and task contrasts for each functional network. Therefore, we believe that computing the predicted-to-actual correlation does not affect our main conclusions.

In conclusion, this study demonstrated a promising probabilistic FC estimation for activity flow mapping, particularly for individual-level predictions. Moreover, our findings revealed divergent influences of areal connectional topology and task contrasts on activity flow prediction across different functional systems. This system-level differentiation aligns with the brain hierarchy, which further corroborates the activity flow mechanism of human cognition.

AUTHOR CONTRIBUTIONS

Hengcheng Zhu: Methodology, Software, Formal analysis, Investigation, Data curation, Writing-original draft, Writing-review & editing, Visualization. **Ziyi Huang:** Investigation, Data curation, Software, Writing-review & editing, Visualization. **Yifeixue Yang:** Investigation, Data curation, Software, Writing-review & editing, Visualization. **Kaiqiang Su:** Investigation, Data curation, Software, Writing-review & editing, Visualization. **Mingxia Fan:** Investigation, Writing-review & editing, Funding acquisition. **Yong Zou:** Investigation, Writing-review & editing, Funding acquisition. **Ting Li:** Investigation, Writing-review & editing. **Dazhi Yin:** Conceptualization, Methodology, Writing-original draft, Writing-review & editing, Supervision, Funding acquisition.

ACKNOWLEDGMENTS

This work was supported by the National Natural Science Foundation of China (31600869 to Dazhi Yin; 81471651 and 11835003 to Mingxia Fan) and the "Technology Innovation 2030-Major Projects" on brain science and brain-like computing of the Ministry of Science and

Technology of China (2021ZD0202600 to Yong Zou). Public datasets were provided by the Human Connectome Project, Washington University–Minnesota Consortium (principal investigators David Van Essen and Kamil Ugurbil) funded by the 16 NIH institutes and centers that support the NIH Blueprint for Neuroscience Research and by the McDonnell Center for Systems Neuroscience at Washington University.

CONFLICT OF INTEREST

The authors declare no competing interests.

DATA AVAILABILITY STATEMENT

The MRI datasets analyzed are available in the Human Connectome Project's ConnectomeDB repository (https://db.humanconnectome.org).

ORCID

Mingxia Fan https://orcid.org/0000-0002-8043-3062
Dazhi Yin https://orcid.org/0000-0002-7461-8220

REFERENCES

Alexander-Bloch, A. F., Gogtay, N., Meunier, D., Birn, R., Clasen, L., Lalonde, F., Lenroot, R., Giedd, J., & Bullmore, E. T. (2010). Disrupted modularity and local connectivity of brain functional networks in childhood-onset schizophrenia. *Frontiers in Systems Neuroscience*, *4*, 147.

Allen, E. A., Damaraju, E., Plis, S. M., Erhardt, E. B., Eichele, T., & Calhoun, V. D. (2014). Tracking whole-brain connectivity dynamics in the resting state. *Cerebral Cortex*, *24*(3), 663–676.

Baker, A. P., Brookes, M. J., Rezek, I. A., Smith, S. M., Behrens, T., Probert Smith, P. J., & Woolrich, M. (2014). Fast transient networks in spontaneous human brain activity. *eLife*, *3*, e01867.

Barch, D. M., Burgess, G. C., Harms, M. P., Petersen, S. E., Schlaggar, B. L., Corbetta, M., Glasser, M. F., Curtiss, S., Dixit, S., Feldt, C., Nolan, D., Bryant, E., Hartley, T., Footer, O., Bjork, J. M., Poldrack, R., Smith, S., Johansen-Berg, H., Snyder, A. Z., … WU-Minn HCP Consortium. (2013). Function in the human connectome: Task-fMRI and individual differences in behavior. *NeuroImage*, *80*, 169–189.

Bassett, D. S., & Sporns, O. (2017). Network neuroscience. *Nature Neuroscience*, *20*(3), 353–364.

Bertolero, M. A., Yeo, B. T., & D'Esposito, M. (2015). The modular and integrative functional architecture of the human brain. *Proceedings of the National Academy of Sciences of the United States of America*, *112*(49), E6798–E6807.

Bertolero, M. A., Yeo, B. T. T., Bassett, D. S., & D'Esposito, M. (2018). A mechanistic model of connector hubs, modularity and cognition. *Nature Human Behaviour*, *2*(10), 765–777.

Bertolero, M. A., Yeo, B. T. T., & D'Esposito, M. (2017). The diverse club. *Nature Communications*, *8*(1), 1277.

Betzel, R. F., Medaglia, J. D., & Bassett, D. S. (2018). Diversity of mesoscale architecture in human and non-human connectomes. *Nature Communications*, *9*(1), 346.

Bijsterbosch, J., Smith, S. M., & Beckmann, C. F. (2017). *Introduction to resting state fMRI functional connectivity*. Oxford University Press.

Biswal, B., Yetkin, F. Z., Haughton, V. M., & Hyde, J. S. (1995). Functional connectivity in the motor cortex of resting human brain using echo-planar MRI. *Magnetic Resonance in Medicine*, *34*(4), 537–541.

Braun, U., Schäfer, A., Walter, H., Erk, S., Romanczuk-Seiferth, N., Haddad, L., Schweiger, J. I., Grimm, O., Heinz, A., Tost, H., Meyer-Lindenberg, A., & Bassett, D. S. (2015). Dynamic reconfiguration of frontal brain networks during executive cognition in humans. *Proceedings of the National Academy of Sciences of the United States of America*, *112*(37), 11678–11683.

Breakspear, M. (2017). Dynamic models of large-scale brain activity. *Nature Neuroscience*, *20*(3), 340–352.

Buckner, R. L., & DiNicola, L. M. (2019). The brain's default network: Updated anatomy, physiology and evolving insights. *Nature Reviews Neuroscience*, *20*(10), 593–608.

Chan, M. Y., Alhazmi, F. H., Park, D. C., Savalia, N. K., & Wig, G. S. (2017). Resting-state network topology differentiates task signals across the adult life span. *The Journal of Neuroscience*, *37*(10), 2734–2745.

Chang, C., & Glover, G. H. (2010). Time-frequency dynamics of resting-state brain connectivity measured with fMRI. *NeuroImage*, *50*(1), 81–98.

Chen, T., Cai, W., Ryali, S., Supekar, K., & Menon, V. (2016). Distinct global brain dynamics and spatiotemporal organization of the salience network. *PLoS Biology*, *14*(6), e1002469.

Cole, M. W., Bassett, D. S., Power, J. D., Braver, T. S., & Petersen, S. E. (2014). Intrinsic and task-evoked network architectures of the human brain. *Neuron*, *83*(1), 238–251.

Cole, M. W., Ito, T., Bassett, D. S., & Schultz, D. H. (2016). Activity flow over resting-state networks shapes cognitive task activations. *Nature Neuroscience*, *19*(12), 1718–1726.

Cole, M. W., Ito, T., Cocuzza, C., & Sanchez-Romero, R. (2021). The functional relevance of task-state functional connectivity. *The Journal of Neuroscience*, *41*(12), 2684–2702.

Cole, M. W., Reynolds, J. R., Power, J. D., Repovs, G., Anticevic, A., & Braver, T. S. (2013). Multi-task connectivity reveals flexible hubs for adaptive task control. *Nature Neuroscience*, *16*(9), 1348–1355.

Corbetta, M., & Shulman, G. L. (2002). Control of goal-directed and stimulus-driven attention in the brain. *Nature Reviews Neuroscience*, *3*(3), 201–215.

Davison, E. N., Schlesinger, K. J., Bassett, D. S., Lynall, M. E., Miller, M. B., Grafton, S. T., & Carlson, J. M. (2015). Brain network adaptability across task states. *PLoS Computational Biology*, *11*(1), e1004029.

de Pasquale, F., Della Penna, S., Sporns, O., Romani, G. L., & Corbetta, M. (2016). A dynamic core network and global efficiency in the resting human brain. *Cerebral Cortex*, *26*(10), 4015–4033.

Deco, G., Jirsa, V. K., & McIntosh, A. R. (2011). Emerging concepts for the dynamical organization of resting-state activity in the brain. *Nature Reviews Neuroscience*, *12*(1), 43–56.

Deco, G., Jirsa, V. K., & McIntosh, A. R. (2013). Resting brains never rest: Computational insights into potential cognitive architectures. *Trends in Neurosciences*, *36*(5), 268–274.

Deco, G., Tononi, G., Boly, M., & Kringelbach, M. L. (2015). Rethinking segregation and integration: Contributions of whole-brain modelling. *Nature Reviews Neuroscience*, *16*(7), 430–439.

Ekstrom, L. B., Roelfsema, P. R., Arsenault, J. T., Bonmassar, G., & Vanduffel, W. (2008). Bottom-up dependent gating of frontal signals in early visual cortex. *Science*, *321*(5887), 414–417.

Engel, A. K., Fries, P., & Singer, W. (2001). Dynamic predictions: Oscillations and synchrony in top-down processing. *Nature Reviews Neuroscience*, *2*(10), 704–716.

Fox, M. D., Zhang, D., Snyder, A. Z., & Raichle, M. E. (2009). The global signal and observed anticorrelated resting state brain networks. *Journal of Neurophysiology*, *101*(6), 3270–3283.

Glasser, M. F., Sotiropoulos, S. N., Wilson, J. A., Coalson, T. S., Fischl, B., Andersson, J. L., Xu, J., Jbabdi, S., Webster, M., Polimeni, J. R., Van Essen, D. C., Jenkinson, M., & WU-Minn HCP Consortium. (2013). The minimal preprocessing pipelines for the human connectome project. *NeuroImage*, *80*, 105–124.

Gonzalez-Castillo, J., Hoy, C. W., Handwerker, D. A., Robinson, M. E., Buchanan, L. C., Saad, Z. S., & Bandettini, P. A. (2015). Tracking ongoing cognition in individuals using brief, whole-brain functional connectivity patterns. *Proceedings of the National Academy of Sciences of the United States of America*, *112*(28), 8762–8767.

Guimera, R., & Nunes Amaral, L. A. (2005). Functional cartography of complex metabolic networks. *Nature*, *433*(7028), 895–900.

Hearne, L. J., Mill, R. D., Keane, B. P., Repovs, G., Anticevic, A., & Cole, M. W. (2021). Activity flow underlying abnormalities in brain activations and cognition in schizophrenia. *Science Advances*, *7*(29), eabf2513.

Hindriks, R., Adhikari, M. H., Murayama, Y., Ganzetti, M., Mantini, D., Logothetis, N. K., & Deco, G. (2016). Can sliding-window correlations reveal dynamic functional connectivity in resting-state fMRI? *NeuroImage*, *127*, 242–256.

Huntenburg, J. M., Bazin, P. L., & Margulies, D. S. (2018). Large-scale gradients in human cortical organization. *Trends in Cognitive Sciences*, *22*(1), 21–31.

Hutchison, R. M., Womelsdorf, T., Allen, E. A., Bandettini, P. A., Calhoun, V. D., Corbetta, M., Della Penna, S., Duyn, J. H., Glover, G. H., Gonzalez-Castillo, J., Handwerker, D. A., Keilholz, S., Kiviniemi, V., Leopold, D. A., de Pasquale, F., Sporns, O., Walter, M., & Chang, C. (2013). Dynamic functional connectivity: Promise, issues, and interpretations. *NeuroImage*, *80*, 360–378.

Ito, T., Hearne, L. J., & Cole, M. W. (2020). A cortical hierarchy of localized and distributed processes revealed via dissociation of task activations, connectivity changes, and intrinsic timescales. *NeuroImage*, *221*, 117141.

Ito, T., Kulkarni, K. R., Schultz, D. H., Mill, R. D., Chen, R. H., Solomyak, L. I., & Cole, M. W. (2017). Cognitive task information is transferred between brain regions via resting-state network topology. *Nature Communications*, *8*(1), 1027.

Kastner, S., & Ungerleider, L. G. (2000). Mechanisms of visual attention in the human cortex. *Annual Review of Neuroscience*, *23*, 315–341.

Keilholz, S., Caballero-Gaudes, C., Bandettini, P., Deco, G., & Calhoun, V. (2017). Time-resolved resting-state functional magnetic resonance imaging analysis: Current status, challenges, and new directions. *Brain Connectivity*, *7*(8), 465–481.

Krienen, F. M., Yeo, B. T., & Buckner, R. L. (2014). Reconfigurable task-dependent functional coupling modes cluster around a core functional architecture. *Philosophical Transactions of the Royal Society of London. Series B, Biological Sciences*, *369*(1653), 20130526.

Kucyi, A., Tambini, A., Sadaghiani, S., Keilholz, S., & Cohen, J. R. (2018). Spontaneous cognitive processes and the behavioral validation of time-varying brain connectivity. *Network Neuroscience*, *2*(4), 397–417.

Liao, X., Cao, M., Xia, M., & He, Y. (2017). Individual differences and time-varying features of modular brain architecture. *NeuroImage*, *152*, 94–107.

Lydon-Staley, D. M., Ciric, R., Satterthwaite, T. D., & Bassett, D. S. (2019). Evaluation of confound regression strategies for the mitigation of micromovement artifact in studies of dynamic resting-state functional connectivity and multilayer network modularity. *Network Neuroscience*, *3*(2), 427–454.

Margulies, D. S., Ghosh, S. S., Goulas, A., Falkiewicz, M., Huntenburg, J. M., Langs, G., Bezgin, G., Eickhoff, S. B., Castellanos, F. X., Petrides, M., Jefferies, E., & Smallwood, J. (2016). Situating the default-mode network along a principal gradient of macroscale cortical organization. *Proceedings of the National Academy of Sciences of the United States of America*, *113*(44), 12574–12579.

Mars, R. B., Passingham, R. E., & Jbabdi, S. (2018). Connectivity fingerprints: From areal descriptions to abstract spaces. *Trends in Cognitive Sciences*, *22*(11), 1026–1037.

Mennes, M., Kelly, C., Colcombe, S., Castellanos, F. X., & Milham, M. P. (2013). The extrinsic and intrinsic functional architectures of the human brain are not equivalent. *Cerebral Cortex*, *23*(1), 223–229.

Mill, R. D., Gordon, B. A., Balota, D. A., & Cole, M. W. (2020). Predicting dysfunctional age-related task activations from resting-state network alterations. *NeuroImage*, *221*, 117167.

Murphy, K., Birn, R. M., Handwerker, D. A., Jones, T. B., & Bandettini, P. A. (2009). The impact of global signal regression on resting state correlations: Are anti-correlated networks introduced? *NeuroImage*, *44*(3), 893–905.

Power, J. D., Cohen, A. L., Nelson, S. M., Wig, G. S., Barnes, K. A., Church, J. A., Vogel, A. C., Laumann, T. O., Miezin, F. M., Schlaggar, B. L., & Petersen, S. E. (2011). Functional network organization of the human brain. *Neuron*, *72*(4), 665–678.

Power, J. D., Schlaggar, B. L., Lessov-Schlaggar, C. N., & Petersen, S. E. (2013). Evidence for hubs in human functional brain networks. *Neuron*, *79*(4), 798–813.

Power, J. D., Schlaggar, B. L., & Petersen, S. E. (2014). Studying brain organization via spontaneous fMRI signal. *Neuron*, *84*(4), 681–696.

Raichle, M. E. (2010). Two views of brain function. *Trends in Cognitive Sciences*, *14*(4), 180–190.

Reid, A. T., Headley, D. B., Mill, R. D., Sanchez-Romero, R., Uddin, L. Q., Marinazzo, D., Lurie, D. J., Valdés-Sosa, P. A., Hanson, S. J., Biswal, B. B., Calhoun, V., Poldrack, R. A., & Cole, M. W. (2019). Advancing functional connectivity research from association to causation. *Nature Neuroscience*, *22*(11), 1751–1760.

Roelfsema, P. R. (2006). Cortical algorithms for perceptual grouping. *Annual Review of Neuroscience*, *29*, 203–227.

Saad, Z. S., Gotts, S. J., Murphy, K., Chen, G., Jo, H. J., Martin, A., & Cox, R. W. (2012). Trouble at rest: How correlation patterns and group differences become distorted after global signal regression. *Brain Connectivity*, *2*(1), 25–32.

Sadaghiani, S., Poline, J. B., Kleinschmidt, A., & D'Esposito, M. (2015). Ongoing dynamics in large-scale functional connectivity predict perception. *Proceedings of the National Academy of Sciences of the United States of America*, *112*(27), 8463–8468.

Sanchez-Romero, R., & Cole, M. W. (2021). Combining multiple functional connectivity methods to improve causal inferences. *Journal of Cognitive Neuroscience*, *33*(2), 180–194.

Shen, K., Hutchison, R. M., Bezgin, G., Everling, S., & McIntosh, A. R. (2015). Network structure shapes spontaneous functional connectivity dynamics. *The Journal of Neuroscience*, *35*(14), 5579–5588.

Shine, J. M., Bissett, P. G., Bell, P. T., Koyejo, O., Balsters, J. H., Gorgolewski, K. J., Moodie, C. A., & Poldrack, R. A. (2016). The dynamics of functional brain networks: Integrated network states during cognitive task performance. *Neuron*, *92*(2), 544–554.

Smith, S. M., Fox, P. T., Miller, K. L., Glahn, D. C., Fox, P. M., Mackay, C. E., Filippini, N., Watkins, K. E., Toro, R., Laird, A. R., & Beckmann, C. F. (2009). Correspondence of the brain's functional architecture during activation and rest. *Proceedings of the National Academy of Sciences of the United States of America*, *106*(31), 13040–13045.

Smith, S. M., Vidaurre, D., Beckmann, C. F., Glasser, M. F., Jenkinson, M., Miller, K. L., Nichols, T. E., Robinson, E. C., Salimi-Khorshidi, G., Woolrich, M. W., Barch, D. M., Uğurbil, K., & Van Essen, D. C. (2013). Functional connectomics from resting-state fMRI. *Trends in Cognitive Sciences*, *17*(12), 666–682.

Song, X. W., Dong, Z. Y., Long, X. Y., Li, S. F., Zuo, X. N., Zhu, C. Z., He, Y., Yan, C.-G., & Zang, Y. F. (2011). REST: A toolkit for resting-state functional magnetic resonance imaging data processing. *PLoS One*, *6*(9), e25031.

Sporns, O. (2013). Network attributes for segregation and integration in the human brain. *Current Opinion in Neurobiology*, *23*(2), 162–171.

Tavor, I., Parker Jones, O., Mars, R. B., Smith, S. M., Behrens, T. E., & Jbabdi, S. (2016). Task-free MRI predicts individual differences in brain activity during task performance. *Science*, *352*(6282), 216–220.

Tik, N., Livny, A., Gal, S., Gigi, K., Tsarfaty, G., Weiser, M., & Tavor, I. (2021). Predicting individual variability in task-evoked brain activity in schizophrenia. *Human Brain Mapping*, *42*(12), 3983–3992.

Uddin, L. Q. (2020). Bring the noise: Reconceptualizing spontaneous neural activity. *Trends in Cognitive Sciences*, *24*(9), 734–746.

Ugurbil, K., Xu, J., Auerbach, E. J., Moeller, S., Vu, A. T., Duarte-Carvajalino, J. M., Lenglet, C., Wu, X., Schmitter, S., Van de Moortele, P. F., Strupp, J., Sapiro, G., De Martino, F., Wang, D.,

Harel, N., Garwood, M., Chen, L., Feinberg, D. A., Smith, S. M., … WU-Minn HCP Consortium. (2013). Pushing spatial and temporal resolution for functional and diffusion MRI in the human connectome project. *NeuroImage*, *80*, 80–104.

van den Heuvel, M. P., & Sporns, O. (2013). Network hubs in the human brain. *Trends in Cognitive Sciences*, *17*(12), 683–696.

Van Essen, D. C., Smith, S. M., Barch, D. M., Behrens, T. E., Yacoub, E., Ugurbil, K., & WU-Minn HCP Consortium. (2013). The WU-Minn human connectome project: An overview. *NeuroImage*, *80*, 62–79.

Vatansever, D., Menon, D. K., Manktelow, A. E., Sahakian, B. J., & Stamatakis, E. A. (2015). Default mode dynamics for global functional integration. *The Journal of Neuroscience*, *35*(46), 15254–15262.

Vidaurre, D., Llera, A., Smith, S. M., & Woolrich, M. W. (2021). Behavioural relevance of spontaneous, transient brain network interactions in fMRI. *NeuroImage*, *229*, 117713.

Vidaurre, D., Smith, S. M., & Woolrich, M. W. (2017). Brain network dynamics are hierarchically organized in time. *Proceedings of the National Academy of Sciences of the United States of America*, *114*(48), 12827–12832.

Wang, R., Liu, M., Cheng, X., Wu, Y., Hildebrandt, A., & Zhou, C. (2021). Segregation, integration, and balance of large-scale resting brain networks configure different cognitive abilities. *Proceedings of the National Academy of Sciences of the United States of America*, *118*(23), e2022288118.

Yin, D., Chen, X., Zeljic, K., Zhan, Y., Shen, X., Yan, G., & Wang, Z. (2019). A graph representation of functional diversity of brain regions. *Brain and Behavior*, *9*, e01358.

Yin, D., & Kaiser, M. (2021). Understanding neural flexibility from a multifaceted definition. *NeuroImage*, *235*, 118027.

Yin, D., Liu, W., Zeljic, K., Wang, Z., Lv, Q., Fan, M., Cheng, W., & Wang, Z. (2016). Dissociable changes of frontal and parietal cortices in inherent functional flexibility across the human life span. *The Journal of Neuroscience*, *36*(39), 10060–10074.

Yin, D., Wang, X., Zhang, X., Yu, Q., Wei, Y., Cai, Q., Fan, M., & Li, L. (2021). Dissociable plasticity of visual-motor system in functional specialization and flexibility in expert table tennis players. *Brain Structure & Function*, *226*(6), 1973–1990.

Yin, D., Zhang, Z., Wang, Z., Zeljic, K., Lv, Q., Cai, D., Wang, Y., & Wang, Z. (2019). Brain map of intrinsic functional flexibility in anesthetized monkeys and awake humans. *Frontiers in Neuroscience*, *13*, 174.

Zalesky, A., Fornito, A., Cocchi, L., Gollo, L. L., & Breakspear, M. (2014). Time-resolved resting-state brain networks. *Proceedings of the National Academy of Sciences of the United States of America*, *111*(28), 10341–10346.

Zamora-Lopez, G., Zhou, C., & Kurths, J. (2010). Cortical hubs form a module for multisensory integration on top of the hierarchy of cortical networks. *Frontiers in Neuroinformatics*, *4*, 1.

SUPPORTING INFORMATION

Additional supporting information can be found online in the Supporting Information section at the end of this article.

How to cite this article: Zhu, H., Huang, Z., Yang, Y., Su, K., Fan, M., Zou, Y., Li, T., & Yin, D. (2023). Activity flow mapping over probabilistic functional connectivity. *Human Brain Mapping*, *44*(2), 341–361. https://doi.org/10.1002/hbm.26044